Updating of geological surfaces during drilling by map migration

Master of Science in Earth Sciences

Muhammad Usman

Department of Earth Science
University of Bergen

January 23, 2023

"The present is theirs; the future for which I really worked, is mine."

Nicola Tesla

Abstract

The accuracy of the geological surfaces in an earth model is dependent on the estimation of the velocities from surface seismic data. The dataset recorded from reverse VSP of the drill bit continuous signal can be utilized to update the velocity model during the drilling. Map migration of geological surfaces through developed algorithms using the new velocity information can improve the geological model ahead of the drill bit and can save well cost.

To this end, this thesis proposes a mapping model for time-to-depth conversion that updates the geological surfaces by using the drill bit seismic waves. Travel time is calculated using ray tracing which is converted to depth using the revised velocities. The thesis methodology is divided into two main parts: the first part calculates the travel time and sampling for the property cube while the second part develops a computational model that converts the interpreted geological surfaces to accurate depth as well as calculates the uncertainty on the updated horizon. This research preprocesses the 2.5D geological model in NORSAR 3D for calculating zero offset two travel time through forward modeling. The velocity model is resampled through linear interpolation after mapping it from the depth domain to the time domain. The interval velocity is integrated over time to calculate the depth for each of the common midpoints (CMP). The proposed model repeats the process with the updated velocity model recorded from the reverse VSP. The revised depth values are compared with the reference depth values calculated from NORSAR 3D. The inputs for the computational model are the geological interpretation (TWT), initial velocity model, and updated velocity model from drill bit seismic waves. This research also explores the effect of uncertainty translated from input datasets to the depth values of the geological surfaces through bootstrapping.

The final results indicate that algorithms developed update the geological surfaces through map migration by utilizing the updated velocity model. The uncertainty translation gives a range of depth variation. The results clearly demonstrate that the mapping model can reduce the rig downtime and eventually save the well cost.

Acknowledgements

This thesis marks the end of my Master of Science degree in Earth Science at the University of Bergen, Department of Earth Science. The thesis was conducted during the year 2022 and has not only been challenging, but also educational and exciting.

I am grateful for the opportunity I have gotten to be able to work with new technology, and state-of-the-art hardware at my disposal at the university, and surrounded by people from several disciplines for continuous support. I would like to give a special thanks to my head supervisor **Einar Iversen** and co-supervisors **Alexander Goertz, Endre Vange Bergfjord** and **Leo Zijerveld** for their excellent support and guidance during the thesis, and much-appreciated feedback throughout the entire master period. furthermore, I would like to thank the **Octio AS** for providing me data set for the research.

I would like to thank my parents for their immense support throughout my degree. I would also like to thank all lecturers and co-students for two exciting years filled with memories and new knowledge.

Contents

Abbreviations

2D	**T**wo - **D**imensional
3D	**T**hree - **D**imensional
TWT	**T**wo **W**ay **T**raveltime
CDP	**C**ommon **D**epth **P**oint
CMP	**C**ommon **M**id **P**oint
VSP	**V**ertical **S**eismic **P**rofile
RMS	**R**oot **M**ean **S**quare
NMO	**N**ormal **M**ove **O**ut
TD	**T**otal - **D**epth

Chapter 1

Introduction

This chapter will give a brief introduction to the motivation behind the development of a computational model that uses the updated velocity model measured from reverse vertical seismic profile (VSP) for time-to-depth conversion. In addition, it will describe the problem and objective of calculating the depth of the reservoir top using the proposed new method. In the last section of this chapter, a brief outline of the thesis is presented.

1.1 Motivation

A seismic survey is typically used to plan a well for hydrocarbons as an initial step. This technique involves multiple steps from acquisition to interpretation and finally planning a well based on the estimated earth model. A geophysicist faces a challenging task when it comes to estimating the velocity of the earth model with the required accuracy. Almost all methods used to estimate velocity are based on seismic travel time inversion [1]. Different methods for estimating the velocity of seismic data have limited accuracy and are affected by multiple factors. Spread length, stacking fold, signal-to-noise ratio, deviations from hyperbolic moveout, and bandwidth can all affect the result [1]. The uncertainty associated with velocity estimation leads to inaccurate depth migration of the target horizon. This results in additional rig time and eventually adds extra cost to the well. In the worst case, the well could be dry if not placed accurately due to the wrong image. Additionally, there can be uncertainty associated with the interpretation of the travel time of the horizons. This uncertainty can arise due to poor resolution of the seismic section, inappropriate seismic processing, or the complexity of the horizons [2]. All these uncertainties are translated into an estimated earth model.

The better velocity model can be estimated by measuring the travel time in situ from the borehole. This is achieved with a Vertical seismic profile (VSP), where sensors

are placed in the well to measure the travel time and interval velocities directly. New velocities migrate the reservoir top more accurately. Compared to the original prognosed depth, this revised calculation of depth provides greater accuracy as the interval velocity is measured directly from the lowermost downhole geophone. The conventional VSP technique is time-consuming and requires the removal of the drill string prior to lowering of wireline VSP array for measurements, resulting in considerable rig downtime. Seismic measurements can be made during drilling using a seismic sensor located in the bottom hole assembly and a known seismic source located on the surface. During the recording process, seismic data is transmitted to the surface using mud pulse telemetry. The repetition of the source point during the connection makes this method more expensive in comparison to drill bit seismic methods [3].

With drill-bit seismic methods, this problem can be overcome by using bit noise as the seismic source. In accordance with the reciprocity principle, a new velocity model can be generated by processing the recorded signal at the surface. The target horizon is migrated to actual depth using software that requires licensing and limited flexibility. The problem raises the possibility of developing an open-source algorithm that is free of charge, scalable, and as effective as commercial software. The new design time-to-depth conversion model could have the capability to take the initial model and update the interval velocities based on the recorded drill bit waves. The proposed model is capable of mapping the target horizon to actual depth, as well as translating uncertainty from input values to revised depth values. The model gives the flexibility to convert travel time values of a single Common depth point (CDP) associated with the well location to all the CDPs present in the study area. Through the application of this model, the uncertainty in depth will be reduced to 5 meters, resulting in a reduction in well costs and a safer drilling process. This computational model will also eliminate the dependency on software for time-to-depth mapping.

1.2 Problem Definition

This thesis focuses primarily on developing a computational model that makes use of the drill bit seismic wave as a source for VSP, thus enabling the reservoir horizon to migrate near an accurate depth. A secondary objective is to visualize the effect of uncertainty on depth associated with the interpretation of the two-way travel time (TWT) and the updated interval velocity model.

1.2.1 Objectives

- To explore the use of the drill bit seismic and velocity updating for map migration of the target horizon.
- To calculate the TWT of the reservoir horizon using an appropriately sampled earth model.
- To develop an open-source model that can do the mapping of the target horizon from the time domain to the depth domain.
- To compare the results of estimated depth using different resampling intervals from the initial model.
- To update the velocity model using the drill bit waves as a seismic source for reverse VSP and revise the depth of the target horizon beforehand.
- To explore the effect of uncertainty translated from the input data (TWT, interval velocity) to the calculated depth.

1.2.2 Proposed Method Overview

Initially, the primary earth model is loaded and sampled for pre-processing. The sampled data is utilized to calculate the zero offset TWT of the target reservoir horizon. These TWT and sampled velocity model is exported for further use as input to the designed computational model for time-to-depth conversion. The model is evaluated based on different resampled values. In order to verify the accuracy of the computational model, the calculated depth values from the designed model are compared to the reference depth values. A reverse VSP data set obtained from the drill bit is then used to update the primary velocity model. Using the updated velocity model, the horizon is remapped in order to estimate an accurate depth. To understand the effect of velocity variation at each cross-line, the migrated depth values are compared with initial depth values. The depth variation range is determined by translating Gaussian uncertainty into output depth values. Figure 1.1 shows an overview of the proposed method.

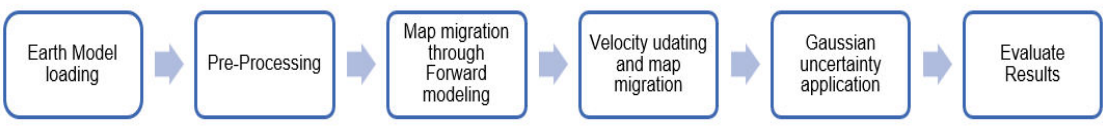

Figure 1.1: A simple overview of the proposed methodology.

1.3 Outline

This thesis begins with a brief introduction and explanation of the motivation behind the concept. The remaining part of the thesis is divided into the following chapters.

- The second chapter, named Background knowledge, illustrates the essential Seismic theory used in the thesis.
- The third chapter, titled Dataset and Pre-Processing, describes the initial dataset and methods for pre-processing the data.
- The fourth chapter is Solution Approach, and it describes the proposed method to update the velocity model and forward model for map migration.
- Chapter five, named Experimental Evaluation and Results, describes and gives a visualization of the obtained results using the proposed forward model before and after velocity updating.
- Chapter six presents a discussion of the achieved results and limitations of the thesis.
- Chapter seven is the last one and presents the conclusions of the work presented in this thesis and recommendations for future work that can be done in this field.

Chapter 2

Background knowledge

Geophysicists and geologists widely use seismic reflection and refraction surveys to image the structure of rock formations beneath the sea floor. This technique is also applicable on land and has been used to determine the subsurface structure worldwide. Seismic reflection methods are a fundamental tool for imaging the Earth's crust and are employed in various marine geology and geophysics studies, as well as for producing images of the subsurface for engineering projects. Moreover, seismic surveys are an integral part of petroleum exploration. It is important to note that seismic surveys vary in terms of the areas covered and, more importantly, the size of the seismic sound source used.

2.1 Seismic Survey

Seismic reflection is the process by which seismic waves are reflected off subsurface boundaries. The reflected waves can then create images of the subsurface structure. Seismic refraction is the process by which seismic waves are bent or refracted when they encounter a boundary between two materials with different acoustic properties. This can be used to determine the depth of the boundary, as well as the velocity of the material above and below the boundary.

Seismic reflection and refraction are used to study the Earth's interior in various ways. For example, seismic reflection can map subsurface structures such as faults, sedimentary layers, and oil and gas reservoirs. Also, it can be used to map the subsurface structure of sedimentary basins, which can be used to determine the basin's age and the type of sedimentary rocks present. Seismic refraction can be used to determine the depth of the Moho (the boundary between the Earth's crust and mantle), to map the velocity of the Earth's crust, which can be used to determine the composition of the crust and the

temperature and pressure at various depths. Seismic reflection and refraction are two of the most important methods used to study the Earth's interior [4].

2.2 Marine seismic

Marine seismic systems involve deploying a sound source behind a vessel, which transmits sound pulses at specific frequencies and intervals. These sound pulses penetrate the ocean floor and propagate through the rock column, producing reflections and refractions when interacting with changes in acoustic characteristics. The returning sound waves are recorded by receivers pulled behind the vessel on a streamer or seismic cable or by seismic recorders deployed on land or temporarily on the seabed (ocean-bottom seismographs). The vessel moves in a straight line at a steady speed, allowing the same area of the seafloor to be recorded multiple times, which can then be synthesized into an image during post-survey processing. Depending on the survey objective, seismic lines are generally shot in groups that intersect, enabling reflectors to be traced from line to line. For scientific purposes, the distance between lines is typically several kilometers, resulting in two-dimensional representations of "slices" through the Earth's crust. These are known as 2-D surveys. In the petroleum industry, 3D seismic is more utilized since the 19's. this technology is very successful in finding hydrocarbon. These 3-D surveys are expensive and require complex technologies.

2.3 Seismic Acquisition

To gain insight into the structure of the Earth's crust, seismic surveys are conducted at discrete, equally spaced shot locations along the survey lines as the survey vessel moves forward with a set speed. This speed is determined based on the survey's depth; deeper surveys require longer intervals for the seismic waves to return, and therefore shots are taken at intervals of 9 to 20 seconds or even 30 to 60 seconds for refraction surveys. The vessel moves at a speed of 4 to 5 knots in such cases. In shallower depths, hydrophone surveys travel faster and have a higher shot rate, although speeds greater than 10 knots can generate ship turbulence along the hydrophone streamer, resulting in noisy data.

2.3.1 2D seismic survey

Two-dimensional (2D) seismic survey techniques employ a seismic cable or streamer, and a single sound source towed behind the survey vessel. It is assumed that the reflections from the subsurface lie directly beneath the survey line along which the vessel sails,

resulting in an image in two dimensions (lateral and vertical). Measurements obtained using streamer sensors are generally less complex than those obtained through 3D or 4D surveys. The streamer and vessel configuration are displayed in Figure 2.1 (A). Owing to the sparse grid of lines and often over a large area, 2D data acquisition lines are usually acquired several kilometers apart [5]. With the help of the 2D lines, interpreters can identify, position, and contour subsurface geologic horizons. However, this technique is flawed due to the knowledge gaps generated by the large distance between grid lines, typically between one and two kilometers. This may lead to difficulty and inaccuracy in estimating the subsurface between sample locations. A majority of this ambiguity and inaccuracy can be eliminated by utilizing 3D data, which has grid lines spaced much closer together.

2.3.2 3D seismic survey

The advent of sophisticated streamer steering and positioning systems in the past two decades has resulted in 3D seismic exploration becoming a standard tool for the hydrocarbon industry. This contrasts with the 2D surveys previously used for academic research, site surveys for engineering purposes, and reconnaissance surveys before a 3D detailed study were conducted. Despite the increased cost of 3D exploration equipment, data capture, and data processing, the quality of information and data obtained is significantly higher than that of 2D seismic data [4]. This is because 3D acquisition covers the full survey area with no gaps between subsurface bins, resulting in data and interpretations that are considerably more precise than those derived from 2D seismic data.

The acquisition of 3D towed streamer seismic data requires the deployment of several parallel streamers, which are pulled by a vessel. A typical 3D seismic acquisition configuration consists of eight to sixteen streamers, two paravanes, eight to sixteen tail and front buoys, and two similar gun arrays with three strings each. The distance between the streamers varies typically between 25 and 200 m. An example of a 3D tow layout with eight streamers and two-gun arrays is shown in Figure 2.1 (B). In this instance, the vessel tows eight 8,000-meter-long streamers. The distance between the streamer and gun arrays is 100 meters and 50 meters, respectively, resulting in a crossline bin size of 25 meters. The minimum offset distance is 300 meters, and the total crossline coverage is 700 meters [4]. To accurately determine their relative and real geographical positions, surficial equipment, such as gun floats, front buoys, and tail buoys, are equipped with GPS transponders. For high-resolution 3D surveys, the lateral spacing between streamers is typically 50 meters.

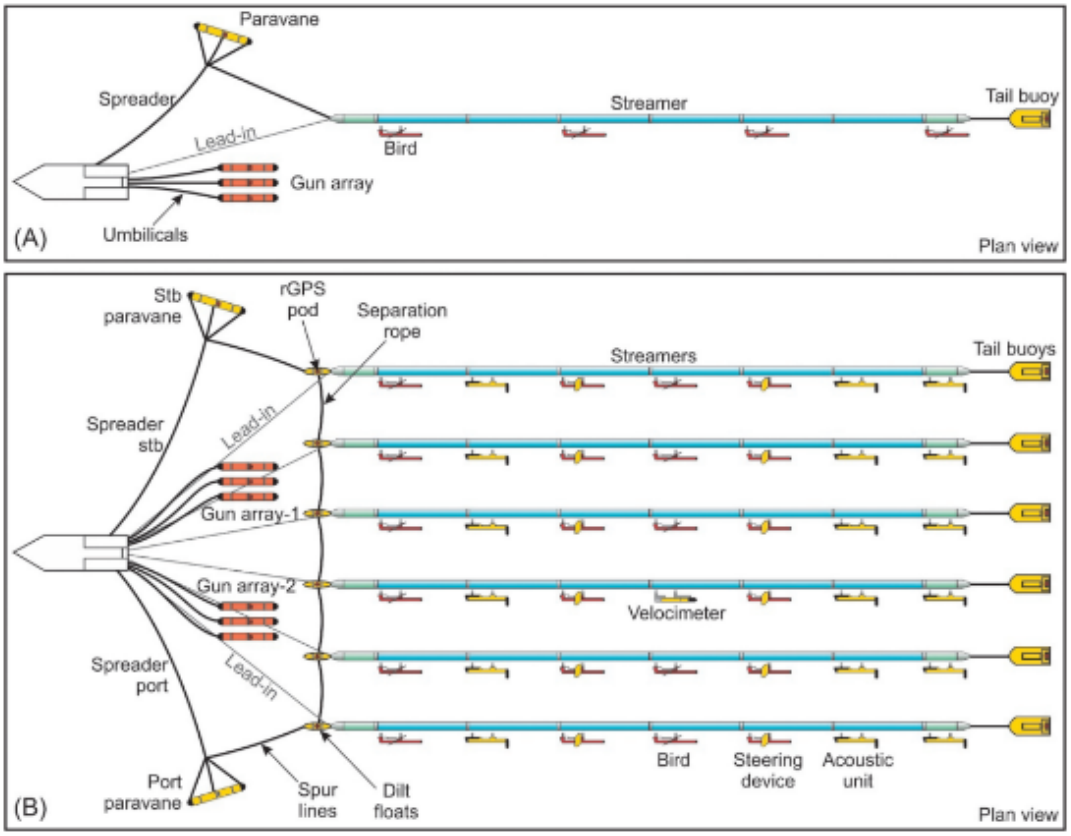

Figure 2.1: Plan view of sea equipment for seismic acquisition. (A) 2D seismic survey geometry (B) 3D seismic survey geometry. This figure is adapted from [4]

2.3.3 Vertical seismic Profile

Vertical Seismic Profiling (VSP) is a widely used technique to obtain time-to-depth information for seismic-well ties. Additionally, processing a VSP survey can provide insights into seismic-wave propagation when combined with sonic measurements. There are three main types of VSP surveys: zero offset VSP, wherein the source is operated from the platform; offset VSP, wherein the source vessel is stationed at a fixed location some distance from the platform; and walkaway VSP, wherein the source vessel traverses one or more lines away from the platform, generating a VSP for each line traverse [5]. The acquisition geometry of different types of VSP is shown in Figure 2.2.

In recent years, the interest in VSP imaging has grown, with numerous onshore and offshore surveys being conducted. It has been observed that the best image results are achieved through 3D VSP surveys using a large VSP array in the well, and a 2D source arrangement acquired using a surface seismic shooting vessel. The shape of the VSP presents its unique challenges and opportunities [6].

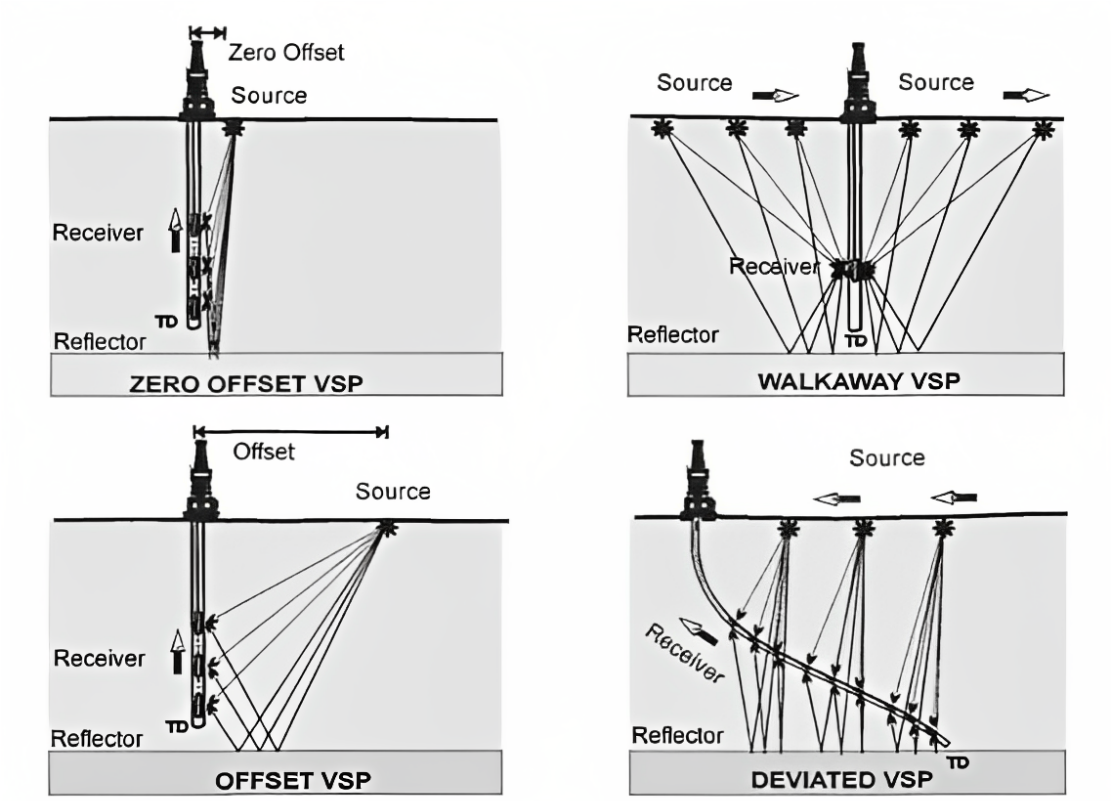

Figure 2.2: Schematic representation of the different types of the VSP acquisition geometries. (A) Zero offset VSP (B) Offset VSP (C) Walkaway VSP (D) Deviated VSP. This figure is adapted from [3]

One of the primary advantages of this method is that the sound wave only travels in one direction through the Earth, resulting in a shorter ray path length and less absorption of higher frequency energy. This allows for greater frequency bandwidth data to be captured. Furthermore, the signal reflected from the reflector is only required to travel a short distance to reach the geophones located downhole. A comprehensive understanding of the geological layers penetrating the well can be obtained by studying drill cuttings and downhole logging data. The combination of better resolution and colocation of the VSP with the well allows the geophysical interpreter to create a highly accurate correlation between the geology and the associated seismic data.

Typically, these surveys last for no more than one or two days. While a few 3D VSPs have been captured, acquiring them was rather costly in history due to the need for multiple passes of the source vessel to get comprehensive 3D coverage. Nowadays, arrays with several 100 or 1000 sensors exist, so shots can be acquired only once, especially when fiberoptic DAS is used. Nevertheless, the problem of rig time remains as all other processes have to be put on hold while performing conventional VSP as the receiver array is in the well. This makes the process comparatively expensive, particularly when the cost of the well time is factored in. This problem rise a need for a process that can be

performed while drilling without disturbing any other process. Here comes the concept of drill bit seismic as reverse VSP that can be performed without any rig downtime.

2.4 Seismic Processing

Data processing is crucial in the geological interpretation of raw field data. It involves a series of steps, often referred to as a processing flow, designed to enhance the data and make it suitable for further analysis. These steps can be broadly divided into three categories: deconvolution, stacking, and migration are shown in the Figure 2.3. In addition to these primary steps, other processing steps are necessary for producing adequate inputs for the primary steps, thereby improving their efficiency. For example, noise removal and signal conditioning are steps often used to enhance the quality of the data before it is subjected to deconvolution, stacking, and migration.

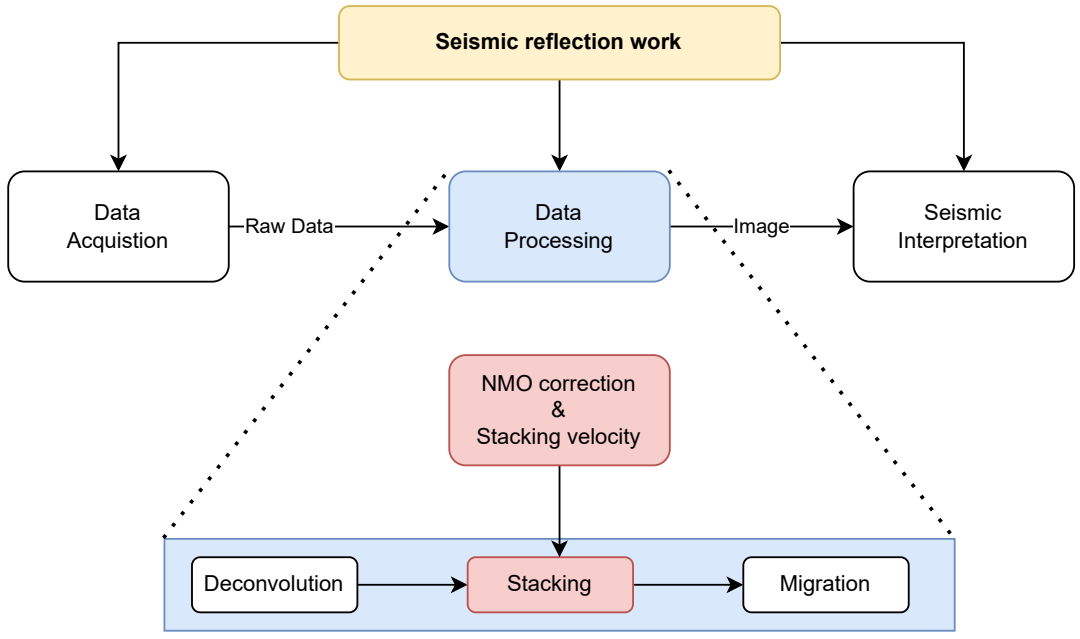

Figure 2.3: Workflow of the seismic reflection survey. Three main steps for processing are also described. This figure is modified from [1]

The seismic data processing procedure is commonly used to generate noise-free input for subsequent deconvolution and to perform velocity analysis for normal moveout (NMO) correction, stacking, and migration. Generally, seismic data processing is used to achieve the following objectives:

- Increasing the signal-to-noise ratio of raw data.

- To present the results in seismic sections, from which subsurface geological information can be derived.

2.4.1 Deconvolution

Seismic exploration of the Earth's subsurface involves the emission of seismic waveforms, or seismic wavelets, as they are known in geophysics. Measurement of the reflected waves is achieved by utilizing pressure or particle-velocity detectors. The process of seismic reflection from the source wavelet W(t) to the receiver is presented in Figure 2.4. The reflected wavefield comprises a series of delayed versions of the input source wavelet and can be calculated from equation 2.1.

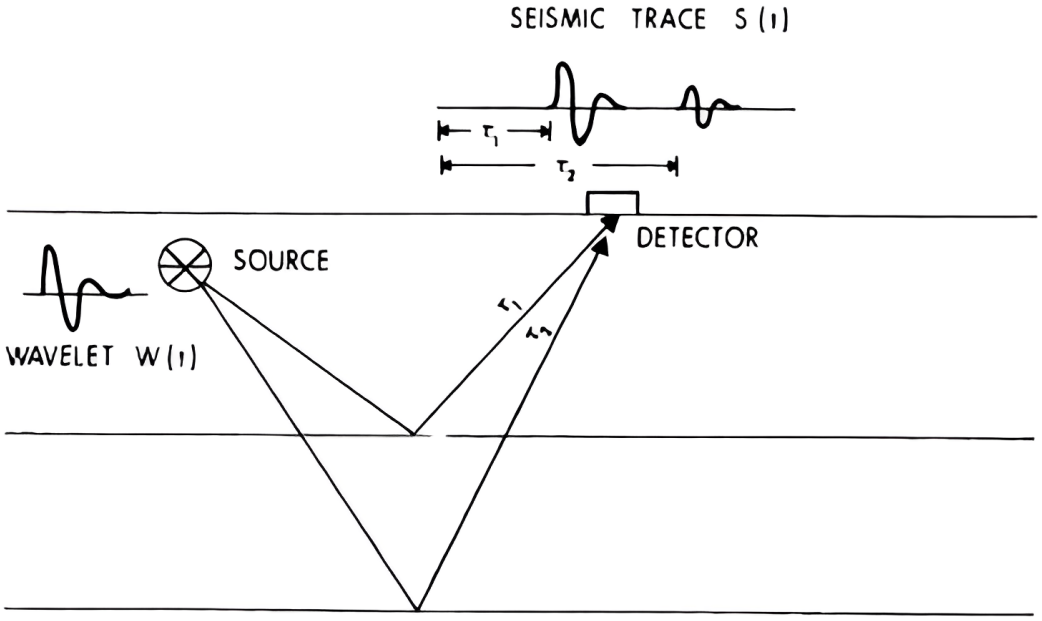

Figure 2.4: Represent the process of seismic recording from source to receiver. The source wavelet is represented with W(t) and the recorded seismic trace with S(t).

The seismic recording can be expressed by a summation of scaled wavelets according to the reflectivity and divergence experienced. This concept is also called the principle of superposition [7]. This process allows us to accurately reflect the seismic data, as the wavelet will adjust accordingly depending on the environment it has encountered (trace) S(t) according to the equation.

$$s\left(t\right) = n\left(t\right) \sum_{i} r_i W\left(t - \tau_i\right) \tag{2.1}$$

The sum of equation 2.1 can be expressed in continuous form as an integral in form of equation 2.2:

$$s(t) = n(t) \int_0^{\infty} r(t) W(t-\tau) d\tau \tag{2.2}$$

Which corresponds to the convolution of the Earth's impulse response r[t] with the seismic source wavelet W(t). This process is known as the convolution integral. A mathematical operation used to calculate the output of a linear time-invariant system given an input signal and the system's impulse response. The convolution process of the source wavelet with the earth reflectivity and resultant signal with noise is displayed in the Figure 2.5. The equation 2.3 represents the convolution of the source signal with the earth reflectivity and the resultant seismic trace. The convolution operation produces a trace that can be used to interpret the subsurface geology of the Earth [8]

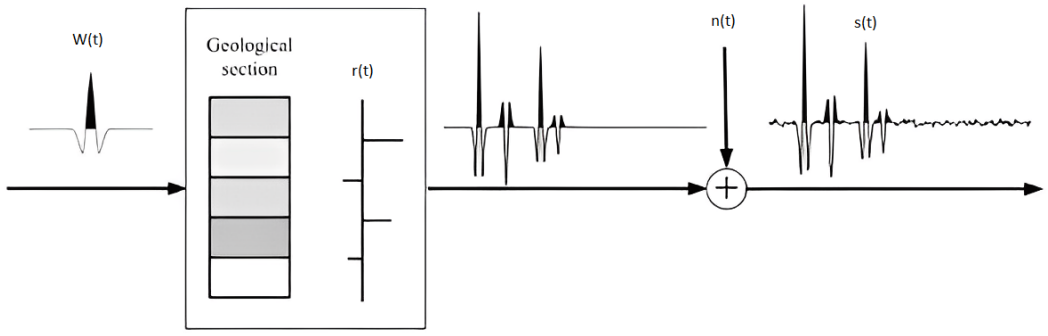

Figure 2.5: Represent the convolution of the source signal w(t) with the earth to make a seismic trace S(t). The noise n(t) is also recorded in the final output signal. This figure is adapted from [8]

$$s(t) = r(t) * W(t) \tag{2.3}$$

Since we are mainly interested in the Earth's impulse response r, we seek a function that removes the effect of w from s, to get a better representation of r. The equation 2.4 can be used to calculate the inverse filter to deconvolve the source signal.

$$f(t) = \delta(t) * \frac{1}{W(t)} \tag{2.4}$$

The filter f is called deconvolution. This is a seismic processing technique to improve temporal resolution and enhance subsurface reflectivity. It involves compressing the fundamental wavelet of the recorded seismogram, reducing reverberations and short-period multiples. Deconvolution is commonly applied both before and after stacking, although if it is not used before stacking, the resulting stack can have a ringing quality that reduces resolution.

2.4.2 Seismic velocities

Seismic velocity is an essential parameter of any seismic survey, regardless of size or type. The normal move out (NMO)is the difference between the zero offset travel time and transit time recorded at offset for a CMP. NMO correction are necessary before stacking which require a stacking velocity. The formula for NMO is mention in equation 2.5.

$$t = \sqrt{t_0^2 + \frac{x^2}{V_{rms}^2}} \tag{2.5}$$

Here t is the two way travel time and t_0 is the zero off set two way travel time and x is the offset distance. Velocity analysis matches the recorded move out and can be improved by employing a semblance plot to select the stacking velocity with the most significant amplitude [1]. These stacking velocities are then used to remove the NMO [9]. To build an effective velocity model, geologic consistency, detailed velocities, and the correct weighting of different types of seismic and well data must be considered [1] [9].

2.4.2.1 Stacking velocity

Stacking velocity is a seismic velocity estimated through a hyperbolic fit of the travel time curve, as Robinson and Coruh (1988) [10] suggested. It is identical to the normal moveout velocity in the case of a horizontally isotropic medium, a concept proposed by Reynolds (2011) [11]. This velocity can be expressed using the equation for travel time, which states that the distance between the source and receiver (x) is equal to the travel time (To) between these two points.

2.4.2.2 Average velocity

The most basic type of velocity is the average velocity, in which we disregard layering and proceed directly to the target horizon as shown in Figure 2.6(a). The average velocity can be calculated through equation 2.6. The total ray path distance must be divided by the overall travel time to calculate the average velocity.

$$V' = \frac{z}{T_0} \tag{2.6}$$

An advantage of this single-layer strategy is that it is straightforward to implement. Since such a model lacks a comprehensive description of the subsurface, it may be less accurate at predicting depths [12].

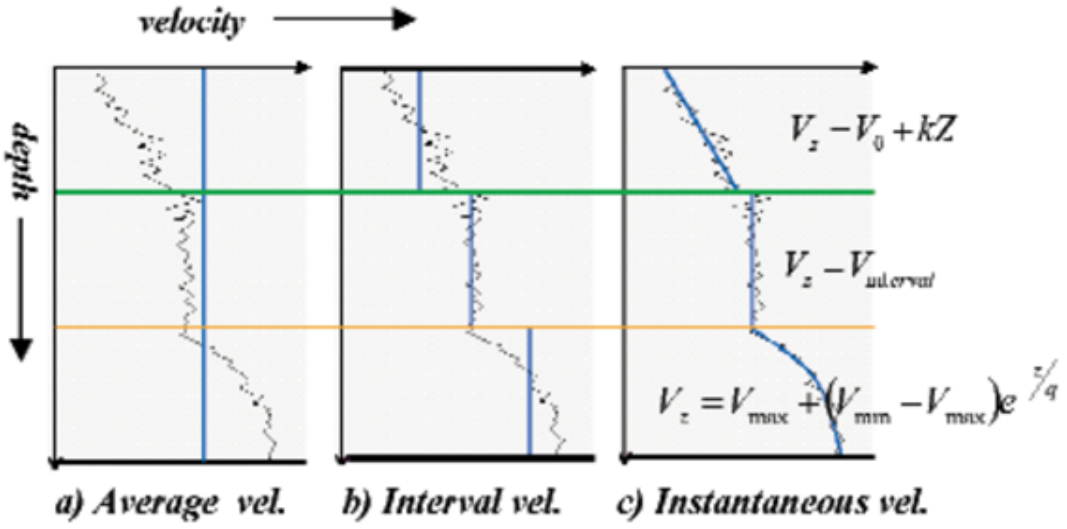

Figure 2.6: illustrate the different types of calculated seismic velocities. (a) is the average velocity (b) is the Interval Velocity and (c) is the instantaneous velocity. This figure is adapted from [12]

2.4.2.3 Root Mean Square(RMS) Velocity

In the case of horizontal layers and normal incidence, the weighted average velocity is known as the root-mean-square velocity (RMS). RMS velocity is often a few percent more than average [11]. Based on the root-mean-square equation 2.7, the velocity is defined as follows:

$$V_{RMS} = \left[\frac{\sum V_i^2 T_i}{\sum T_i}\right]^{\frac{1}{2}} \tag{2.7}$$

It is important to note that Vi represents the interval velocity, and ti means the two-way transit time of the ith layer.

2.4.2.4 Interval velocity

Velocity applied to defined depth intervals is known as interval velocity as shown in Figure 2.6 (b). Compared to interval velocity, average velocity provides less information regarding velocity fluctuation in the subsurface. To calculate it, divide the layer thickness Zi by the interval transit time (ti) as mentioned in equation 2.8.

$$V_i = \frac{z_i}{T_i} \tag{2.8}$$

The Dix Formula (Dix, 1955) can be used to determine the interval average of the nth layer.

2.4.2.5 Dix equation

Interval velocities (Vint) are determined by calculating the time difference between the two chosen horizons on a seismic section using the seismic equation. Additionally, the horizon-consistent stacking velocity profiles of the layer boundaries are used to calculate the interval velocity profiles through the Dix conversion [1]. The equation 2.9 is the Dix equation for calculating the interval velocities.

$$V_n = \sqrt{\frac{V_n^2 T_n - V_{n-1}^2 T_{n-1}}{T_n - T_{n-1}}} \tag{2.9}$$

In this equation 2.9, vn represents the isotropic interval velocity in the layer bounded by the (n-1)th layer boundary above and the nth layer boundary below, tn and tn-1 are the two-way zero-offset times, and Vn and Vn-1 are the RMS velocities. While the stacking velocities are typically assumed to represent the real root-mean-square velocities, it may be necessary to adjust them for the effects of the dip in some cases. Equation (1) assumes that the layer interfaces are flat and that the offset range used to estimate the RMS velocities Vn and Vn-1 corresponds to a small dispersion. Despite this, Dix conversion cannot provide an entirely accurate estimate of interval velocity. As noted by Yilmaz (2001), the interval velocity profiles generated via Dix conversion can often exhibit sinusoidal oscillations resulting from oscillations in the stacking velocity profiles[1].

2.4.2.6 Instantaneous velocity

The instantaneous velocities can be calculated by employing a time-depth curve derived from a vertical seismic profile. A check shot survey or an integrated sonic log is shown in Figure 2.6 (c). This type of curve is characterized by variations in velocity over very small depth changes, which is why it is called an instantaneous curve. [12]. proposed that the most suitable linear model to describe such fluctuations is a function of depth. Equation 2.10 presents the mathematical expression for the instantaneous velocity.

$$V_{(z)} = v_0 + kz \tag{2.10}$$

Specifically, V(z) represents the instantaneous velocity at depth Z, while V0 and k represent the line's intercept and slope.

2.4.3 Stacking

In seismic exploration, stacking combines traces from multiple shot records into a single output trace. It is an essential step of the seismic data processing and imaging workflow. By combining the traces corresponding to different shot-to-receiver distances, we can obtain a trace with an improved signal-to-noise ratio for a particular common midpoint. Stacking multiple single-shot traces can enhance the subsurface illumination in seismic imaging. Among the numerous steps in seismic data processing, common-midpoint (CMP) stacking is the most important one. It can differentiate signal from noise with the same frequency and hence improve the signal to noise ratio (SNR) of the resulting trace as shown in Figure 2.7. This can facilitate the interpretation of the seismic data.

Harry Mayne's CMP technique, established in 1962, has been widely used as a standard for recording and processing reflection data. The model postulates two components of a seismic record: the signal and the noise. According to the model, the signal is aligned and similar in shape to the signal on other recordings. In contrast, the noise is statistically independent of the signal and any other record and has a mean value of zero [13].

The sample values corresponding to a certain two-way time of all traces in a CMP gather are added and then divided by the total number of samples added [14]. The following equation 2.11 can sum up this fundamental procedure:

$$A\left(t\right) = \frac{1}{N}\sum_{i=1}^{N} a_i\left(t\right) \tag{2.11}$$

Where A(t) represents the sample value of the stacked trace at two-way time t, N represents the fold of the stack, and $a_i\,(t)$ represents the sample value on trace i at two-way time t.

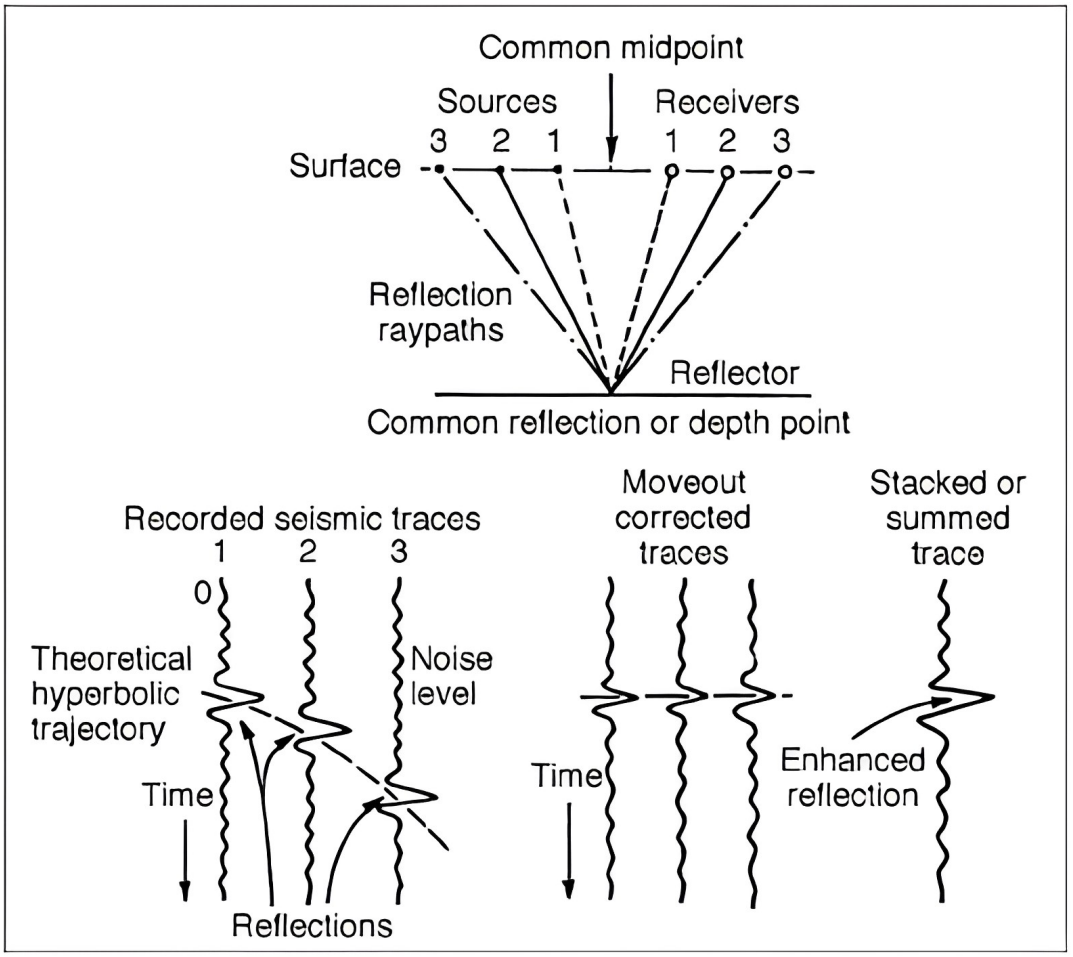

Figure 2.7: Represent the process of stacking the reflection signal for a single CMP. Stacked trace is enhanced and has less signal-to-noise ratio. The figure is adapted from [15]

Combining multiple well-aligned traces makes it possible to amplify the effective signals and reduce the Gaussian white random noise. However, when the noise is powerful and the number of traces available for stacking is limited, simple summation may not suppress the random noise. Various stacking strategies have been developed that are more effective in low signal-to-noise ratio (SNR) conditions [14]. One such technique is principal component analysis (PCA) based stacking, which is a powerful way to improve the effectiveness of seismic stacking [16].

2.4.4 Seismic Migration

Migration is the process of reconstructing a seismic section to accurately represent the Earth's reflectivity map, as recorded by seismic data collected at the surface. Seismic waves detected by a receiver are a combination of waves traveling from multiple subterranean directions. This means that most recorded events are from geological formations far away from the receiver, not from reflectors directly underneath [17]. Migration increases the lateral resolution of the seismic section by gathering energy from the Fresnel zone and combining diffraction patterns from point reflectors and faulted beds.

The structural distortion of anticlines and synclines observed in non-migrated sections is the effect of ray bending and the incidence angle that the reflection point from a dipping reflector is at a different lateral position than the CMP obtained from stacked trace. On non-migrated seismic sections, Synclines within which the reflector curvature exceeds the curvature of the incident wavefront are represented by a 'bow-tie' event (as shown in Figure 2.8) resulting from the existence of three separate reflection sites for any surface position [9].

Wave equation migration (WEM) is a contemporary migration model which uses seismic wave equations to recreate the wavefield near a reflecting interface. This technique effectively traces the wavefield backward through time, allowing for the reconstruction of the geometry of the reflector. The wavefield of a reflection event is propagated halfway back in time, resulting in the wavefield being placed at the reflecting interface [9]. The wave equation is an essential tool for migration models in contemporary seismology. The wave equation is a partial differential equation that describes the motion of waves within a medium due to a wave source. This type of migration is known as wave equation migration and is a critical component of many seismic migration models [18].

One form of migration employed is the finite difference method, which approximates the wave equation by means of a computer-solvable equation. In contrast, frequency-domain migration involves using Fourier transformations to solve the wave equation. The required spatial changes are conducted in the frequency domain and then retrieved by inverse Fourier transformations [9].

Migration of seismic sections through direct modeling of ray paths and estimations of the ground can be an effective method of obtaining accurate reflection periods. In this method, the geometry of the reflecting interfaces is constantly adjusted to eliminate any discrepancies between the calculated and observed reflection periods. The Kirchhoff method is a data migration technique based on diffraction search and energy transfer along the diffraction curve to its crest. Kirchhoff is increasingly ineffective with steep reflectors, and it is independent of the signal-to-noise ratio [19].

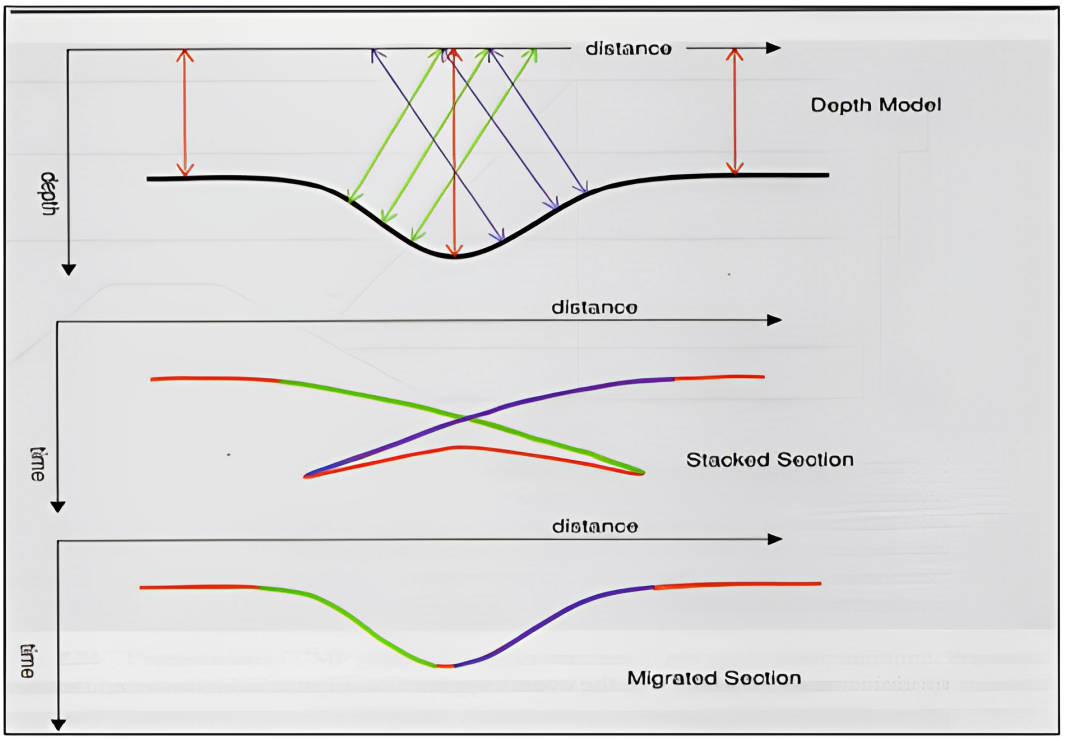

Figure 2.8: Represent the stacked signal for the syncline. The stacked section makes a bow-tie effect. The lower part shows the migrated section of the syncline. This figure is adapted from [20]

2.5 Time-to-depth conversion

Converting seismic reflection data from the time domain to the depth domain is a critical step in subsurface interpretation. This conversion is based on a direct geophysical relationship that requires knowledge of the subsurface velocity to calculate the depth [21]. Time to depth conversion is based on simple equation 2.12.

$$d = vt \tag{2.12}$$

In case where the velocity is variable, the equation can be extended into integral form as equation 4.3. By utilizing this conversion, the seismic section can be effectively integrated with geological, petrophysical, and production data. TWT records from the surface are suitable for a range of subsurface interpretations and will provide an accurate picture of the subsurface structure.

Seismic wave velocity is a fundamental concept for accurately determining a reflecting plane's depth, slope, and thickness [22]. The velocity modeling process, which establishes a correlation between depth and seismic time (TWT), is one of the most crucial components

of converting seismic data into depth [12]. Various approaches to constructing a velocity model depend on the objectives and available data sources. In the case of the migration process, obtaining the stacking velocity as a function of the NMO (normal moveout) is often necessary, even though velocity data are not derived from measurements but rather from the NMO correction through trial and error [23]. The time-to-depth conversion technique typically involves the following steps:

1. By utilizing time migration techniques, a series of time horizons can be extracted from an image volume. These time horizons are typically associated with layer interfaces with velocity contrast or geological structures. Identifying and interpreting these time horizons is necessary to understand the image volume's geologic structure better.

2. The next step in the process is to obtain a horizon-consistent RMS velocity map. This is achieved by intersecting the RMS velocity functions over the survey area with the time horizons, as previously interpreted. These RMS velocity functions are derived from prestack time migration gathers. This intersection ensures that the RMS velocity map is consistent with the time horizons interpreted in the previous step.

3. The next step after obtaining the RMS velocity maps is to apply Dix conversion to convert them into interval velocity maps. Dix conversion is a method used to convert RMS velocities into interval velocities using the equation 2.9. This process can be repeated for each RMS velocity map until an interval velocity map is generated.

4. Utilizing vertical-ray or image-ray depth conversion techniques with the interval velocity maps produced in step (3) to generate depths for the time horizons produced in step (1).

Constructing an initial model based on the time-to-depth conversion involves combining interval velocity maps derived from step (3) with depth horizons from step (4). This initial model can be further calibrated and adjusted by introducing well data to generate depth structure maps for well location (Ylmaz 2001). Furthermore, the predicted initial model can be employed to perform 3-D post- or prestack depth migration and generate a depth image volume [1].

2.6 Seismic Interpretation

Interpreting seismic data is a complex process that requires a deep understanding of the fundamental geophysical assumptions involved [24]. It is assumed that the coherent events observed on seismic records reflect the acoustic impedance contrasts in the subsurface, which are associated with distinct formations and geometries [24]. However, errors in seismic interpretation may arise due to a number of factors, including errors in data acquisition and processing [25]. Therefore, it is important to consider the potential sources of error when interpreting seismic data to ensure accurate results.

The interpretation of seismic data involves the identification of structural elements and the separation of discrete stratigraphic units. This process is based on the analysis of folds and faults, which are the most significant characteristics of a seismic structure. Further information can be obtained through seismic facies analysis, which evaluates several parameters: reflection amplitude, frequency, polarity, continuity, configuration, the morphology of seismic facies units, and interval velocity [26]. This information can then be used to determine the geological characteristics of the subsurface.

2.7 Reservoir modeling and drilling

To develop and produce hydrocarbon reserves, reservoir modeling is becoming increasingly significant. Measurable data are interpolated or extrapolated based on geologic interpretations derived from seismic data and an understanding of sedimentary processes to generate comprehensive reservoir descriptions. These technologies provide information that can be incorporated into reservoir models. The structural frameworks outline the principal compartments of a reservoir and usually provide first-order controls on fluid volumes in place and fluid flow during production [27]. It is, therefore, essential to model structural frameworks with precision . There are specific reasons for creating high-resolution three-dimensional models:

- It is necessary to estimate the original hydrocarbon volume of the reservoir accurately. These in situ volumes are crucial for determining the economic viability of extracting a particular reservoir.
- Well, locations must be chosen in a manner that is commercially optimal and stable in light of the uncertainty associated with reservoir descriptions.
- Through the use of flow simulations, reservoir performance can be forecast under different production scenarios. The economics of several alternatives can be compared to determine the optimal number of wells and parameters for operation.

- It is essential to make critical decisions even though there is considerable unpredictability: how many wells should be drilled? Well locations? When do the injection and infill wells come into play?

The formulation of a reservoir model depends on the model's objective and the data available. A model can be built to plan wells, estimate volumes, perform simulations, or model seismic activity [28]. The availability of data also influences a reservoir model. A schematic representation of the various types of relevant data required for reservoir modeling is provided in Figure 2.9 [29].

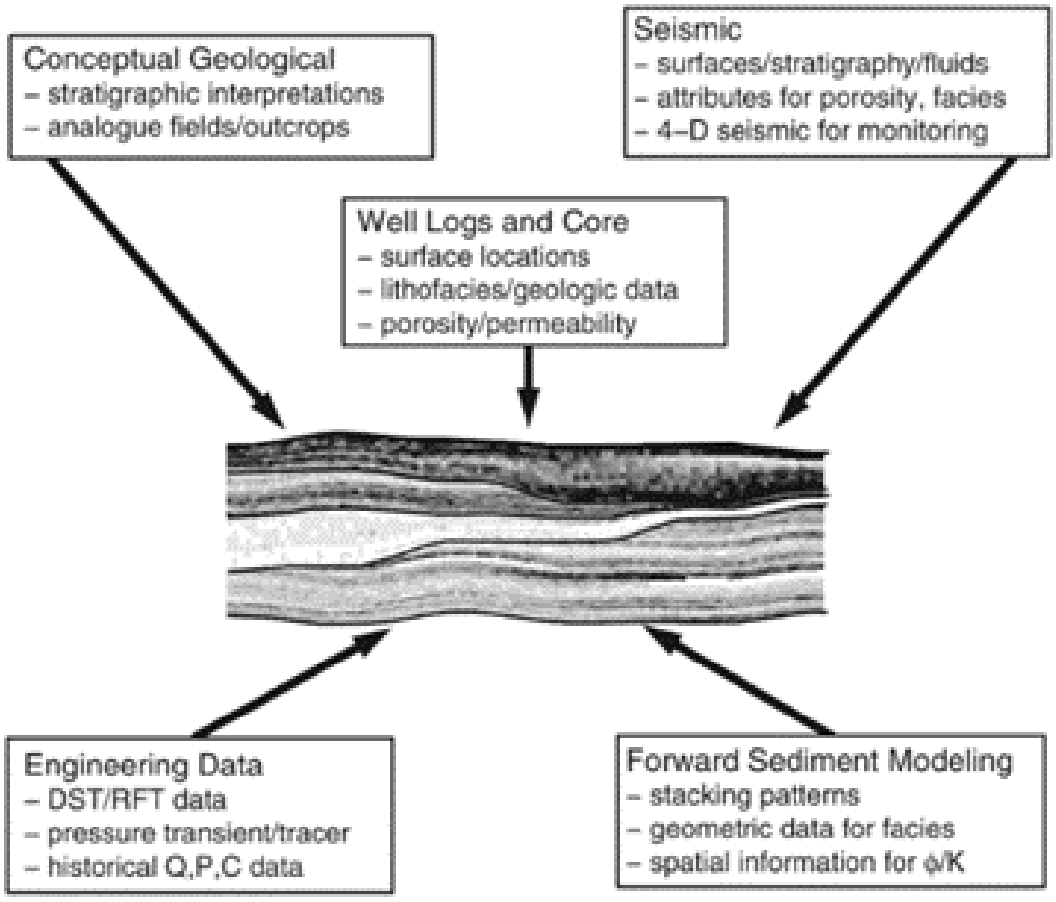

Figure 2.9: Image in the center represents the complex 3D reservoir model generated by combining all the data from different sources. [29]

2.7.1 Well Planning

Planning a well is one of the most challenging and complex tasks in drilling engineering. Planning a well involves developing a safe, economic, and feasible approach to drilling in light of various factors. Unfortunately, it is not always possible to achieve these objectives in each well due to geological and seismic limitations [30]. Costs associated with good

drilling include drilling and completion expenses. A relationship between the depth of the well and the cost of drilling the well is presented in equation 2.13 [31]:

$$C_{drill} = -39 \times 10^{-8} d^3 + 4.00 \times 10^{-4} d^2 - 0 \cdot 84d + 903d \tag{2.13}$$

Where d represents the depth of the well in meters and Cdrill represents the drilling cost per well in 2005 dollars. This is the case for onshore drilling and offshore drilling cost will be much higher. Changing the depth of the target horizon can significantly impact the well's price.

The planning of a well is a process that requires contributions from both geoscience and engineering personnel. To create an effective well plan, the first step is to determine the depths of the casings and cement them. The drilling engineer must consider geological factors, such as the formation pressure and fracture mud weight, as well as any potential issues the hole may pose. Formation pressure, or pore pressure, can significantly affect the design of the well. If the pressure is normal, no further planning challenges present themselves. However, additional casing strings must be used to protect the low-pressure areas if subnormal pressure is encountered. This is done to prevent the weight of the drilling mud from fracturing the formation at the last casing seat [3]. This process is illustrated in Figure 2.10. Therefore, during subnormal pressure conditions, it is essential to ensure the hole is drilled and cased to the correct depth, allowing drilling to proceed without difficulty.

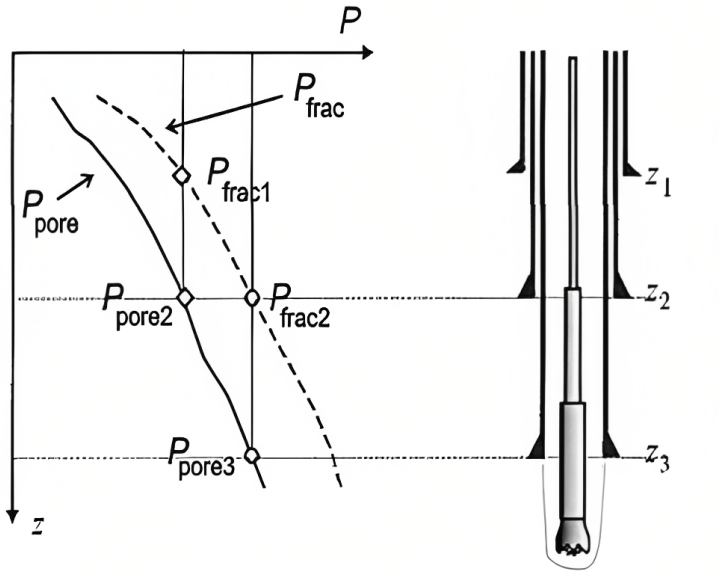

Figure 2.10: Represent the graph of pore-pressure and fracture pressure on the left. A well section and its relation of the casing with the pressure is illustrated on the right. This figure is adapted from [3]

2.8 Seismic while drilling

The seismic recording of a drilling operation is made by recording the vibrations caused by the drilling bit and the wavefields generated by the bit as a source. In the passive drill-bit seismic approach, the drill-bit noise is a source of seismic activity. A reciprocal VSP and normal VSP configuration are illustrated in Figure 2.8. Following the reciprocity principle, a reciprocal VSP obtains equivalent seismic results. It is stated that data collected from wells and surface seismic sources correlate with information obtained from drill-bit sources and surface receivers [3]. It is necessary for both the source and the receiver to maintain the same orientation while shifting depth to satisfy the reciprocity criteria. The SWD data are compared to the surface seismic sections to optimize depth interpretation and provide information while drilling.

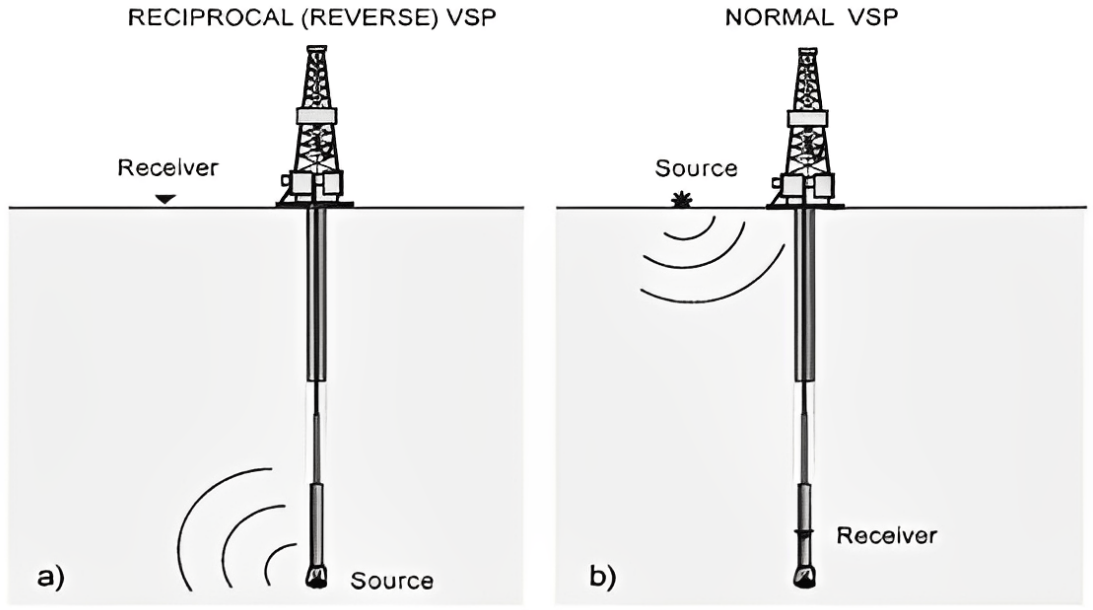

Figure 2.11: illustrate the difference between the normal and reverse VSP. (a) is the reverse VSP and (b) is the normal VSP. This figure is adapted from [3]

Calculations have demonstrated that the drill-bit seismic source emits an adequate amount of radiated energy and that the frequency bandwidth is broad enough for correlation in SWD applications. The novel interferometry approach used to acquire high-quality zero offset data makes this method more trustworthy regarding depth conversion and looking ahead during drilling [32]. This technique allows to place the arbitrary number of receivers at the surface and hence a 3D VSP can be acquired.

Chapter 3

Dataset and Pre-Processing

This chapter explains the dataset which is used for this project. It also gives an overview of all the steps of the pre-processing of the dataset.

3.1 Geological model scenario

For this thesis, a synthetic model of the sub-sea from the North Norwegian Sea is used as the input model as shown in Figure 3.1. The model is created in the NORSAR suite in the depth domain based on the initial velocity information. The interval velocities are defined between the horizon blocks and fault planes. Table 3.1 provides information regarding depth horizons, interval velocities, and their respective intervals. Typically, the target reservoir horizon lies under the unconformity to which the target horizons are onlapping. The Upper Jurassic shale above the target horizon is pinched out towards the unconformity. The horizons below the Upper Jurassic are truncated by an unconformity and the horizon is dipping away from the unconformity. The input geological model is initially a 2.5D model, which means that the 2D model has been extended into the third dimension. This extension assumes that there is no variation in depth and interval velocities in the third dimension. A geological model in depth domain and interval velocities are required as input values for this thesis project. Considering the complexity of the Fulmar horizon, the Top upper Fulmar horizon is selected as the target horizon.

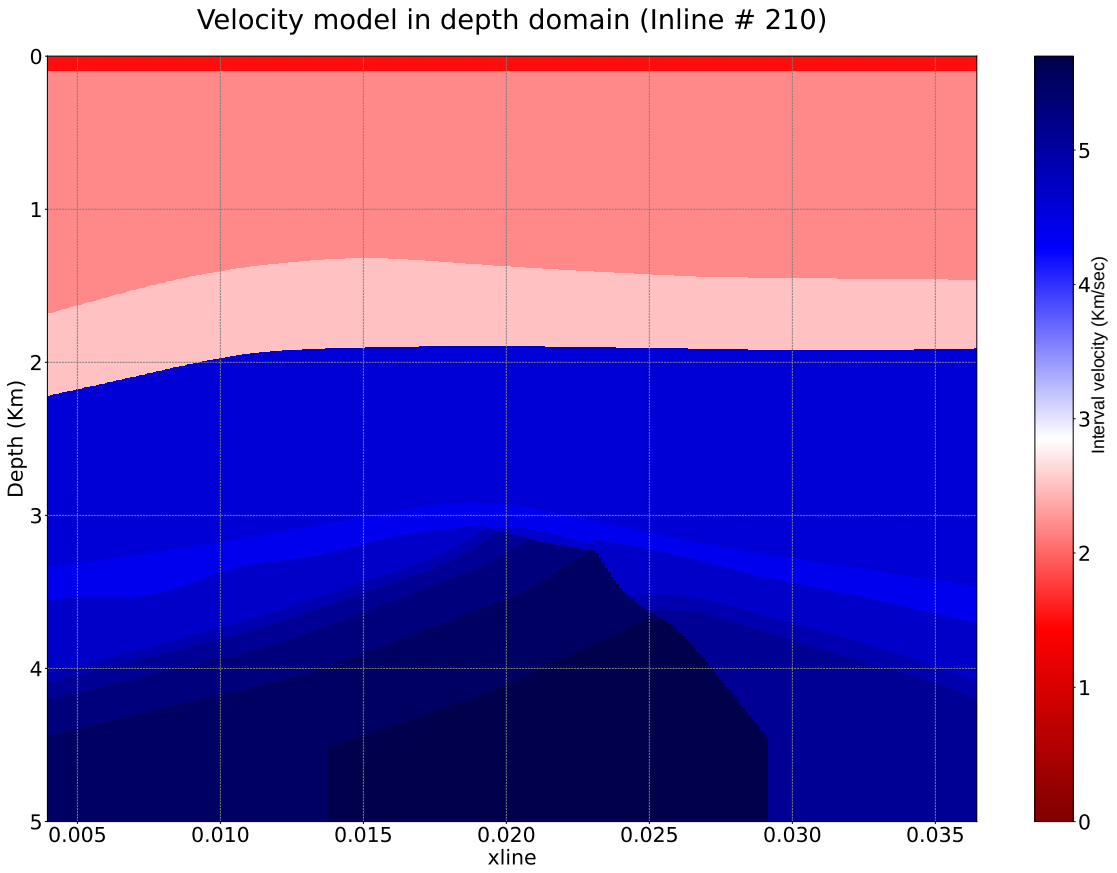

Figure 3.1: Intial Velocity model represents different geological surfaces and their associated interval velocities. This model is provided by Octio AS.

Table 3.1: Represents all the horizons and their associated blocks. Interval velocity (Vp) associated with each block is presented in Km/sec

Horizons	**Blocks**	**Input Interval Velocity (Vp) Km/s**	**Updated Interval Velocity (Vp) Km/s**
Sea Floor	Sea Water	1.5	1.5
Seabed			
Top Paleocene	Overburden	2.2	2.2
Top Chalk	Paleocene	2.5	2.5
Top Cromer Knoll	Chalk	4.6	4.6
Base Cromer Knoll	Cromer Knoll	4.4	3.3
	Upper Jurassic Shale	4.7	3.1
Top Upper Fulmar	Upper Fulmar	4.9	4.9
Base Upper Fulmar	Base Fulmar	5.1	5.1
	Pentland	5.3	5.3
Top Skagerak	Triassic Skagerak	5.5	5.5
Top Shale	Triassic Shale	5.7	5.7

3.2 Model Pre-Processing

This section describes the steps involved in pre-processing the dataset used in this thesis to migrate maps. This process depends on the model that has been provided as initial input. In this project, a SEG-Y file of the initial model is provided which has velocity and depth information of the faults and the horizons. Following is a description of how pre-processing operations are performed in order to generate the desired dataset from the given data.

3.2.1 Travel Time Measurements

For time-to-depth mapping, two-way time travel is required as input. Due to the fact that the initial model is in the depth domain, no direct travel time information is provided for the target horizon. Two-way travel time can be calculated using forward modeling. With the help of NORSAR software, travel time is calculated based on the information (interval velocity and depth) provided by the initial model. An "interactive ray tracing" module is used with "image ray tracing" shooting for this purpose. The method determines the normal incident travel time of the selected surface by tracing the ray from the source to the common depth point (CDP) on the target horizon and back to the receiver. Figure 3.2 shows the transmission of rays from the source to the common depth point. Through the "grid generation" module in NORSAR 3D, a time surface is generated which includes travel time data along with their associated in-line & cross-line numbers and XY-coordinate. The transit time remains the same before and after updating the velocity.

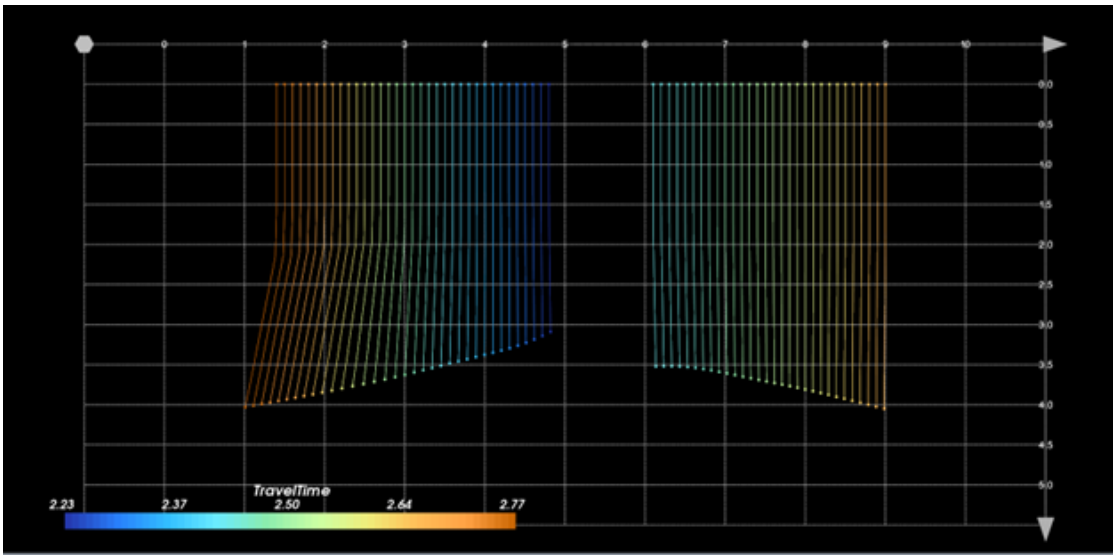

Figure 3.2: Represent the calculated TWT of the target horizon. The straight line represents the ray traveling from the source to the common depth point (CDP) and back to the receiver.

3.2.2 Data sampling

Performing this step on the initial data is the first and most significant step. The process of resampling is very sensitive since it can affect the depth of the target horizon. Sampling intervals are determined by the type of model (2D, 2.5D, or 3D), as well as the threshold for the depth of the target horizon. All three dimensions of the initial model are sampled and the sampling interval is specified in Table 3.2. By sampling these values, a property cube is created that contains velocity information along with in-line and cross-line numbers. The initial velocity model is derived from this property cube in the SEG-Y file. The updated Velocity model is sampled in a similar manner and the property cube is extracted for later use.

Table 3.2: Presents the sampling interval and the number of resampled values from the initial velocity model.

Data	Sampling interval (Km)	Total sample
in-line (Y-axis)	0.1	5
cross-line (X-axis)	0.025	325
Interval velocity (Z-axis)	0.001	5001

3.2.3 Depth Conversion

The sole purpose of this step is to create a reference against which the converted depth results will be compared. The time horizon is converted to depth using the property cube generated in section 3.2.2. The time horizon is converted to depth because the software does not have any functionality that can export the original depth horizons from the geological model. The converted depth values are the benchmark to verify the algorithms that will be written in the thesis. Time-to-depth conversion is performed using NORSAR's "Time to Depth" module. Data is stored as a depth horizon in a tri-mash file that contains depth value for CDPs and their associated XY coordinates.

3.3 Data Extraction

Once all this preprocessing has been completed, the next step is to extract the files that can be used in the mapping algorithms. It is important to note that all extracted values should share at least one common value that can be used to compare values. A common value may be a combination of in-line and cross-line information or XY coordinates.

The software contains three types of files that must be extracted. As a first step, a text file is exported with the TWT data. There are several components in this file, including XY coordinates, in-line cross-line data, and TWT. In the next file, the property cube is exported, and the data is exported in the form of the SEG-Y (special format for seismic) file format. With the help of special libraries, the SEG-Y file is further processed in the algorithms in order to use it for numerical calculations. The last dataset exported is the depth data of the target horizon which will be used to compare the results calculated through algorithms. This data is also exported in text format but only has XY coordinates and depth information.

3.4 Data QC and filtering

It is necessary to conduct a quality control check on these numerical values before using them. In the TWT of the target horizon, there are some extremely high values that need to be filtered out before they can be used in the codes. A higher value appears when there is no surface data available for the survey area. The TWT is sorted according to the in-line values after these values have been filtered. Due to the fact that the model is 2.5D, only one in-line data is required for the project. The algorithm for the 3D model may be repeated in order to use all of the sorted in-line data. Tri-mash data,

which includes depth information, is also sorted in accordance with XY coordinates. The coordinates are correlated with in-line & cross-line data to compare the depth values provided by the software and are calculated based on the algorithm.

Chapter 4

Solution Approach

4.1 Introduction

This chapter explains the detailed methodology adopted during the thesis for generating the computational model for time-to-depth conversion. In the first section, each step of the computational model is explained and the last section describes the software and all the libraries used in algorithms. Figure 4.1 gives a detailed overview of the adopted methodology.

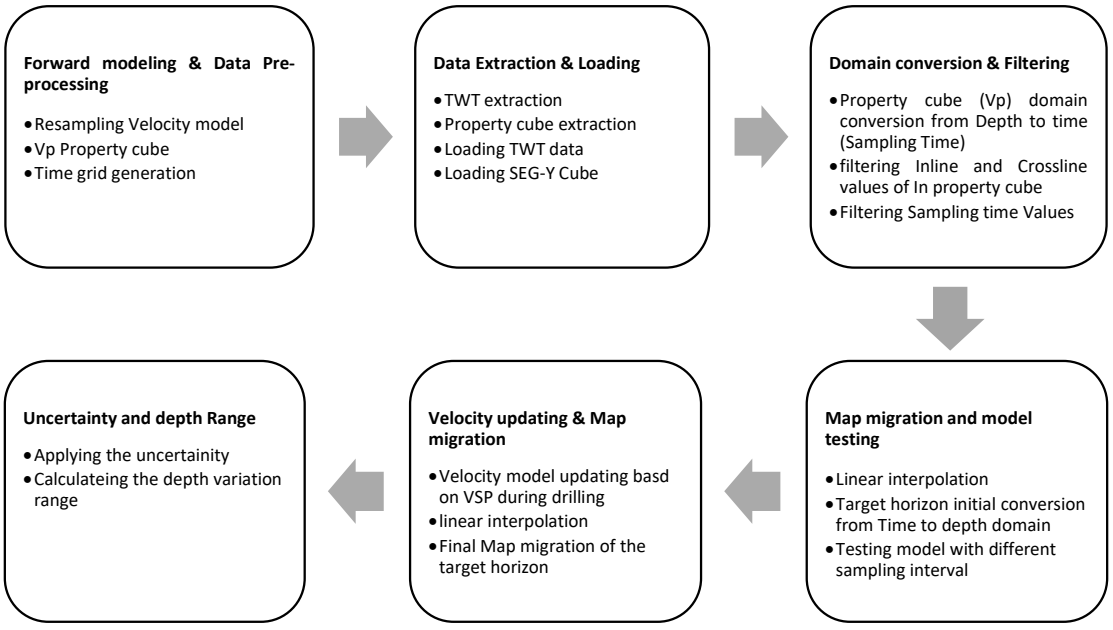

Figure 4.1: A detailed overview of the methodology adopted through the project.

4.2 Time to depth mapping model

This mapping model is inspired by Einar Iversen's (2021) forward model for time-to-depth conversion. The original forward model was simple and needed to be modified in order to accommodate complex horizons. This thesis presents a computational model that can handle complex horizons and can take SEG-Y files as input for velocities. Figure 4.2 shows the workflow of the new designed model. In this case, the computational model has been applied to a set of 2.5D data based on the available input data. The time-to-depth conversion model is described below in terms of its different functionalities

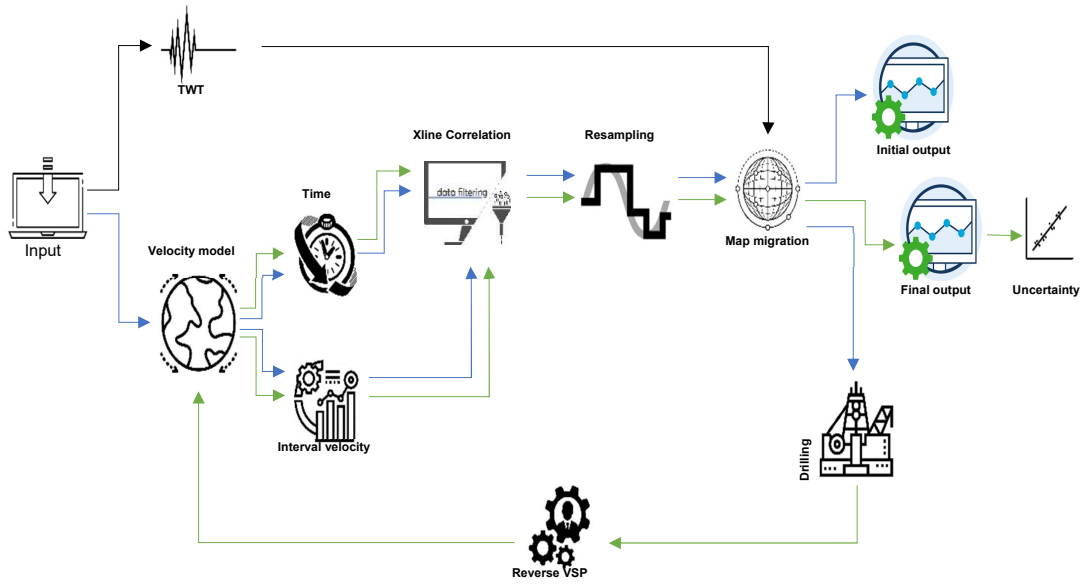

Figure 4.2: A workflow of the designed computational model for time to depth conversion through reverse VSP. Blue arrows represent the time-to-depth conversion before drilling and green arrows represent the time-to-depth conversion after drilling.

4.2.1 Time to depth Mapping

The first step in the computational model is to convert the input velocity model extracted from NORSAR 3D into a time domain model. It is important to note that these algorithms are very specific to the input dataset. Due to the fact that the subsurface model used in this application is in the depth domain which must be transformed into the time domain. This is accomplished by extending a simple equation of motion to convert the velocity model into the time domain. Considering the time (t_0) to be zero when the depth (z) is zero, equation 4.1 takes the average velocity and change in depth to calculate the time (t_i) for every depth (z_i).

$$\Delta \, z = \bar{v} \Delta t \tag{4.1}$$

Here Δz is the change in depth, $\bar{v}$ is the average velocity and Δt represents the change in time. The above equation 4.1 can be expanded to new equation 4.2 to calculate the time as

$$t_i = t_{(i-1)} + \Big(\big(z_i - z_{(i-1)}\big) \,/\, \Big(\big(v_{(i-1)} + v_i\big) \times 0 \cdot 5\Big)\Big) \tag{4.2}$$

This equation 4.2 calculates the time values and the resultant velocity model is a function of time. Figure 4.3 presents the initial and resultant functions against sample numbers for single in-line and cross-line. In figure 4.3, the blue line represents sampling depth, while the orange line corresponds to sampling time. It is apparent from the calculated time values that the sampling interval is not constant for the time function. The sampling interval is varying in accordance with the interval velocity. This problem rises the need for resampling with a constant sampling interval.

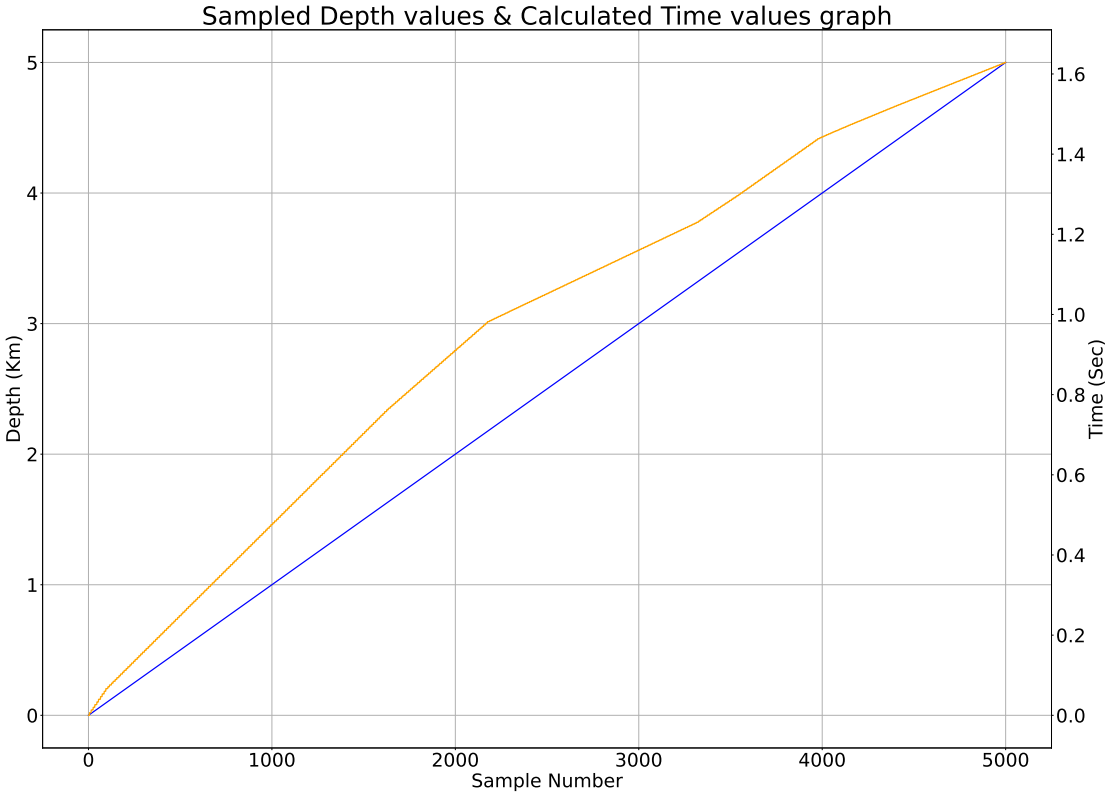

Figure 4.3: Represent graph of sampled depth values and calculated time values. The blue line represents the depth values against the sample number while the orange line represents the time values against the sample number. The depth sampling interval is constant and the time sampling interval varies.

4.2.2 Linear interpolation

The mapping of velocity models from depth to time disturbs the sampling interval, which must be equally spaced. Thus, it is necessary to resample the sampling time values and corresponding velocity values for each cross-line. The linear interpolation algorithms developed by Einar Iversen (2021) are utilized in order to achieve this objective. Using linear interpolation, it is easy to resample interval Velocity and corresponding sampling time with different sampling intervals by linearly interpolating the values. For each cross-line, resampling of sampling time and associated interval velocity is carried out separately in this model. The mapping model's computational time can be affected by the resampling interval, which may increase or decrease the number of resampled values. It is important that the resampled values are consistent with the initial velocity values.

4.2.3 In-line/cross-line correlation

Subsurface geology is not straightforward, rather it is complex and discontinuous. It is often the case that horizons are truncated either by faults or by lithological pinch-outs. In order to overcome this problem, each cross-line number is correlated with the corresponding cross-line number in the velocity model. Cross-lines having no TWT data of the target horizon are eliminated from the input dataset. The process is subject to a target horizon. It is quite possible that all cross-lines in the velocity model have TWTs for the CDP on the subjected horizon. A velocity value associated with correlated cross-lines is extracted using this process, as well as the sampling time associated with those cross-lines. Those values will be used as inputs for the next step.

4.2.4 Time to depth conversion

In the mapping model, this process represents the centric point that is used for time-to-depth conversion. TWT is actually converted into depth by using the time to depth conversion algorithms designed in this section. Equation 4.3 represents the extended form of the equation of motion and is used in this process. Velocity is a function of time ($v\,(t)$) in the input velocity model. As time changes, velocity changes as well. In equation 4.3, the interval velocity is integrated over time. It integrates the associated velocity for each cross-line from time zero to the travel time of the CMP. As the travel time is in two ways so, the equation is multiplied by half. For each cross-line, this process will be repeated in order to calculate the depth values.

$$z = \frac{1}{2}\int_{t=0}^{t=T} v\,(t)\,dt \tag{4.3}$$

4.3 Horizon depth comparison

In this step, the model is tested by comparing the depths of the converted horizon with the tri-mash values exported from the software. This process gives the opportunity to evaluate the resampling time interval used for the linear interpolation in the model. The sole purpose of the step is to test the time-to-depth conversion model with different resampling intervals. The resultant depth values are compared with the reference depth of the synthetic geological model exported from the NORSAR 3D. The time-to-depth conversion model is tested with an increasing number of resampled values.

4.4 Velocity updating

This is the most significant and central aspect of the thesis. The main idea behind the concept is to use the drill bit as a seismic source in order to update the velocity by reverse VSP. Seismic waves are recorded through the ocean bottom cable surrounding the well. During the drilling process, the bit produces waves that are the source of the reverse VSP. The recorded waves are processed as zero offset VSP in real-time in order to construct the seismic-to-well tie and to calculate the exact depth of approaching the target horizon. [32]. As a result of these newly processed velocities, the initial model is updated. Prior to drilling the horizon, the same mapping model used previously is applied again to convert the time horizon into an accurate depth.

4.5 Uncertainty implementation

As a result of the updated velocity model, the target horizon is mapped close to its actual depth. However, there is a possibility that all three input variables (TWT, Interval velocity and its associated time) may be subject to some uncertainty. It is expected that there will be uncertainty in the picking of the TWT of the target horizon. In a similar manner, even after updating the reverse VSP velocity, some errors may exist in the velocity and sampling time. These expected uncertainties are expressed as Gaussian errors. In order to calculate possible depth values, the model is iterated based on random values within the limits of the applied uncertainty. Due to the random nature of the certainty calculation, the 95% and 67% confidence intervals are applied which limits the possibility of outliers. This process translates the applied uncertainty into depth values. The process is based on Bjarte's (2021) algorithms and codes have been modified according to time-to-depth mapping.

4.6 Experimental tools

This section of the thesis describes the details of the software and different libraries used for data loading and processing.

4.6.1 NORSAR Suite (3D)

Travel time is calculated using NORSAR 3D since the initial synthetic model is designed with this tool. The NORSAR 3D software is used for modeling seismic rays in three dimensions utilizing an open ray model. It is an advanced version of the NORSAR that allows a 2D model to be expanded into a 2.5D model. In addition to its ability to exchange data with other programs, this software can also extract data in numerous formats, such as SEG-Y, Ascii, and TRX [33]. In order to compute zero offset TWT from source to receiver for the target horizon, an image ray tracing module is utilized. This algorithm was developed by researchers at NORSAR [34].

4.6.2 Python

In this thesis, Python is used as the programming language. Python is a well-designed programming language that can be applied to real-world applications. It is a general-purpose programming language that is high-level, flexible, and object-oriented. The object-oriented style of programming of Python simplifies the process of writing clear, logical code for small to large-scale applications that is also easily understandable [35]. In addition, it is open source and there are no restrictions on its use, modification, or distribution. Scripts written in Python are compatible with all operating systems [36].

4.6.2.1 Numerical Python

The Numerical Python library (NumPy) is an open-source library for the programming language Python. Multidimensional array objects are provided for advanced mathematical operations and state-of-the-art scientific and commercial research and development. Many operations are performed with this library, including extensive complex computations, random number generators, linear algebra algorithms, and Fourier transformations, among others [37].

4.6.2.2 Segyio

The Segyio library facilitates the interaction with seismic data in both SEG-Y and Unix formats. This library was created by Equinor ASA and is an open-source, user-friendly, and community-oriented seismic application library. This library supports the reading and writing of header and trace data in binary, trace, and textual formats. Segyio is closely integrated with NumPy, and the library offers MATLAB and Python bindings. The objective of this module is to facilitate the transformation of seismic data into NumPy arrays that can then be used for further processing and manipulation.

4.6.2.3 Matplotlib

Matplotlib provides a comprehensive and powerful Python toolkit for building static, dynamic, and interactive visualizations. In other words, it is a plotting module for the Python programming language together with its NumPy extension for numerical analysis. It is capable of displaying publication-quality plots, ranging from simple 2-dimensional graphs to sophisticated 3-dimensional images [38]. Typically, most of the work is performed within the pyplot submodule. In this thesis, all three-dimensional figures are drawn using the Axes3D submodule of the Matplot toolkit.

Chapter 5

Experimental Evaluation and Results

In this chapter, the experiments and their results are produced using the proposed methodology. For the purpose of this thesis, only one horizon is considered to be the top of the reservoir. A visual representation of the results is also provided in this chapter.

5.1 Target Horizon

The target horizon in this thesis is the reservoir top. This is the ultimate horizon upon which the planning and drilling of the well are based. In this thesis, the target horizon is the Top Upper Fulmar. The horizon is complex, with the anticlinal shape and flanks dipping away from each other. The Horizon is truncated by two faults. Due to faulting, both flanks are separated from one another and the horizon is missing from the crust. A pre-processed target horizon can be seen in Figure 5.1. This horizon is plotted on the basis of the in-line and cross-line location, and the color scale shows how the travel time values vary. At the extreme ends of the horizon, the ray has the longest travel time, whereas, in the middle, the ray has the shortest travel time. As the original model was 2.5D, the represented horizon does not show any variation in the in-line (y-axis). This thesis uses only data associated with one of the in-lines in order to limit the data used.

5.2 Model Testing

The algorithms of time-to-depth conversion are tested by passing the initial subsurface model. Based on the designed computational model, values are converted from time to depth by passing through multiple stages. Detailed explanations of the results obtained from each step are provided below.

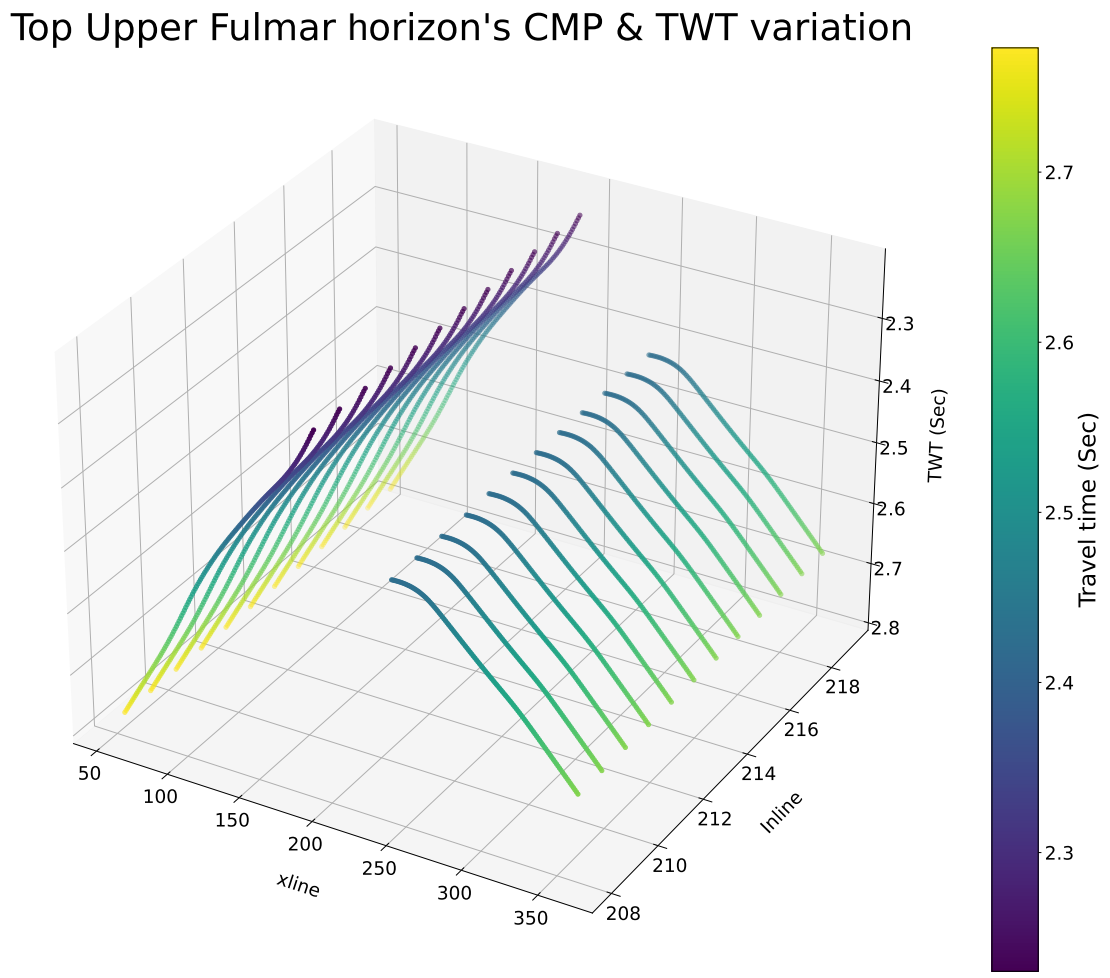

Figure 5.1: illustrate the target horizon common depth point location in 3D. The color bar shows the travel time variation on each CMP.

5.2.1 Resampling through linear interpolation

The interval velocity and associated time are resampled at a different sampling rate. The sampling rate affects the consistency of the interval velocity as a function of time. The sampling interval depends on the number of values to be extracted. Figure 5.2 and figure 5.3 show plots of time vs interval velocity before and after resampling for the cross-line number 363. A new sample of 501 values was taken from 5001 initial values in Figure 5.2. The reduced resampled interval velocity shows inconsistency with the initial velocity. To make the resampled values more consistent with the initial values, the resampling interval is reduced. Figure 5.3 represents the 3501 resampled values from the original dataset. Each of the cross-lines has a different sampling interval in order to get the same number of resampled values. As a result of the fine sampling rate, the initial and resampled data points are more consistent. Changes in consistency of the resampled time values with different sampling intervals are shown in Appendix A A

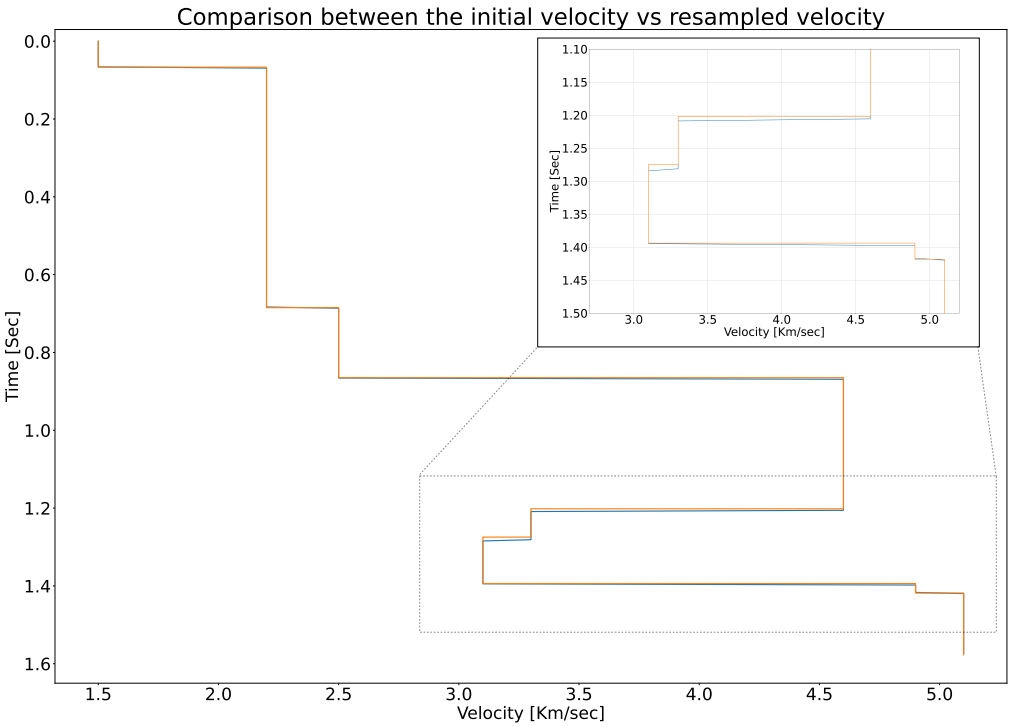

Figure 5.2: Represent inconsistency between Depth vs resampled Velocity & Depth vs initial velocity. The 501 values are resampled from the 5001 original values. In the upper right corner, a zoomed section is also displayed.

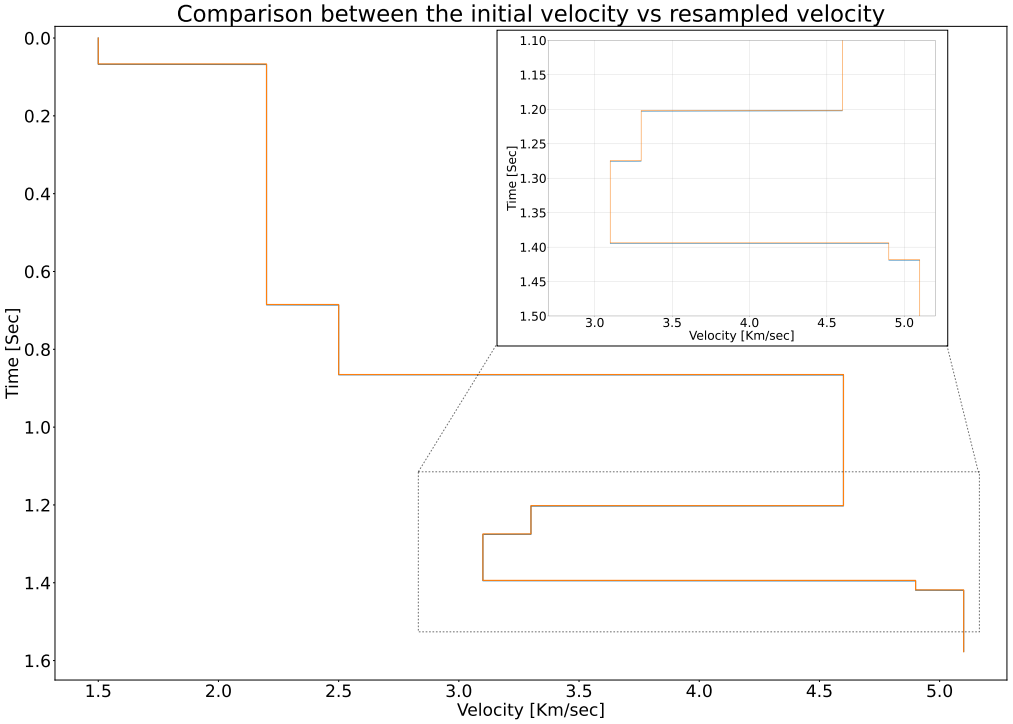

Figure 5.3: Represent consistency between Depth vs resampled Velocity & Depth vs initial velocity. The 3501 values are resampled from the 5001 original values. In the upper right corner, a zoomed section is also displayed.

5.2.2 Time to depth conversion

The time-to-depth conversion algorithm is used to translate the TWT of the target horizon into depth. Based on resampled interval velocities, the Top Upper Fulmar horizon is converted to depth. With the coarsely sampled interval velocity model (number of samples = 501), the depth values of the horizon are undulated as shown in Figure 5.4. Comparing this converted Top Upper Fulmar with the reference depth values indicates that they are not in agreement. Calculated depth values differ slightly from the target horizon's reference depth values. By reducing the resampled interval and taking more samples through linear interpolation, the depth difference is reduced. Figure 5.5 illustrates a reduction in undulation and the depth values become closer to their reference values. At the deepest point, the depth difference is 0.0005 kilometers, while at the shallowest point, it is 0.003 kilometers. Through the computational model, the depth conversion improves as the resampling interval is reduced. The testing results of the computational model with different resampled values are shown in Appendix B B. There is a trade-off with the increased number of values. Increasing the number of resampled values from 501 to 3501 increased the processing time from 5 minutes to 20 minutes.

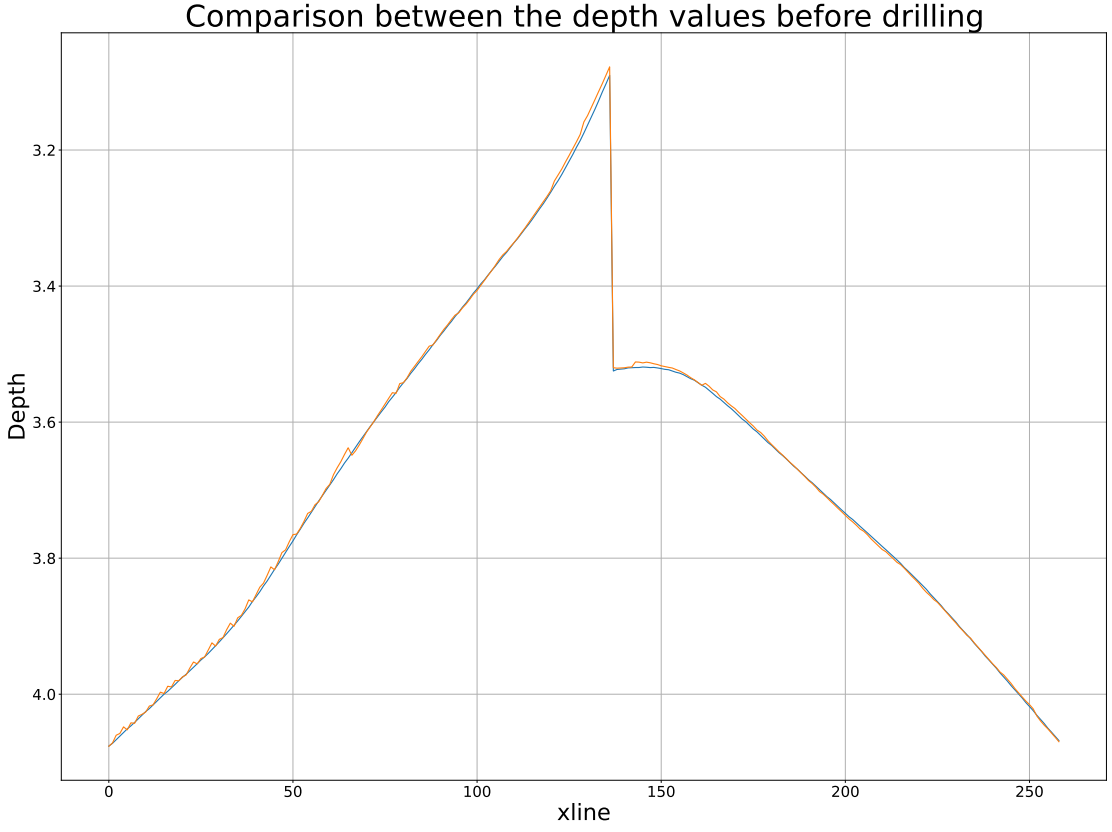

Figure 5.4: Represent results from time-to-depth conversion (orange) with the original horizon (blue) obtained from NORSAR which serves as a reference. The depth values are calculated with 501 resampled velocity values.

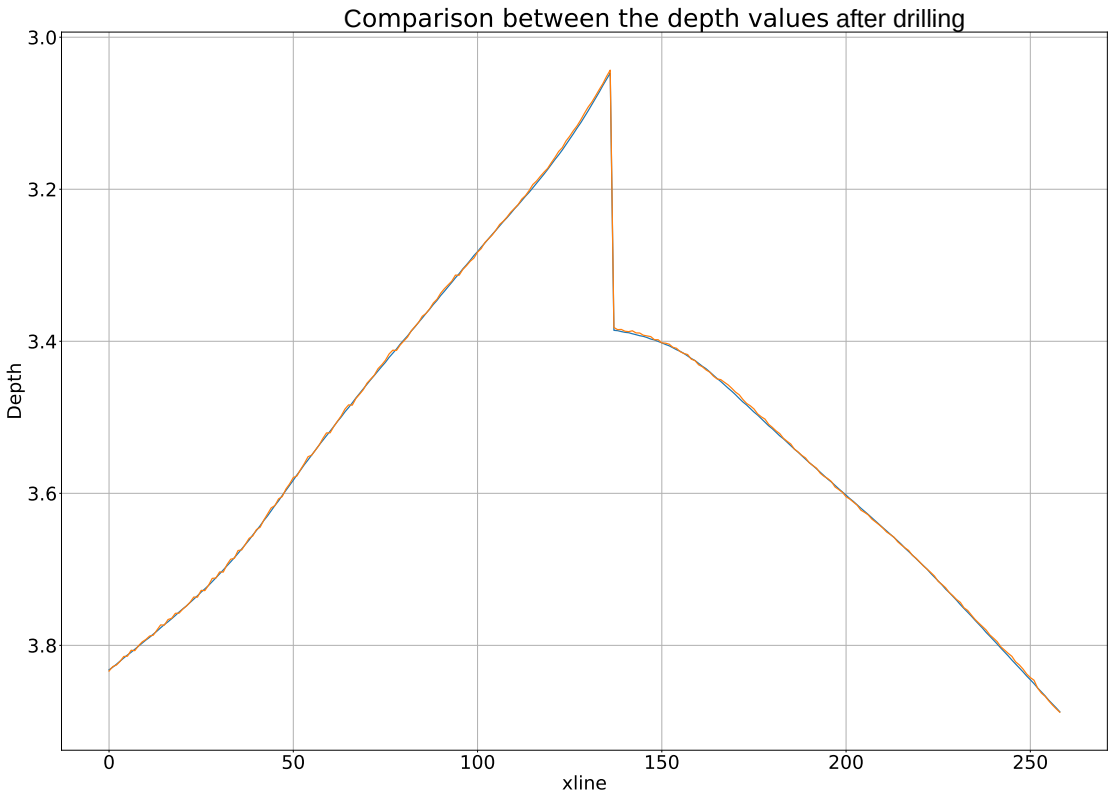

Figure 5.5: Represent results from time-to-depth conversion (orange) with the original horizon (blue) obtained from NORSAR which serves as a reference. The depth values are calculated with 3501 resampled velocity values.

5.3 Drilling and Reverse VSP

As a proof of concept, we conduct here a hypothetical experiment under the assumption that the initial velocity model, which has been obtained from surface seismic data only, is improved in accuracy by VSP data obtained during the drilling of the well in parts of the overburden. The recorded interval velocities during drilling are identical to the initial input velocities in the Overburden, Top Paleocene, and Top Chalk blocks. As drilling progresses, the recorded interval velocities in the Cromer Knoll and Upper Jurassic Shale are different from their initial input velocities. During reverse VSP in the Cromer Knoll block, an interval velocity of 3.3 km/sec has been recorded, which was originally calculated as 4.4 km/sec from surface seismic data. In the Upper Jurassic shale, the interval velocity has been revised from 4.7 km/sec to 3.1 km/sec. Figure 5.6 represents the updated velocity model recorded during the drilling. The inversion (reduction) in velocities in the Cromer Knoll block is difficult to estimate from the surface seismic data and expected to be measured more accurately with the reverse VSP. Still, the well is not drilled through the target yet. This approach shows how far the target horizon is

still away from the current depth of the well so the drilling can proceed with an updated depth.

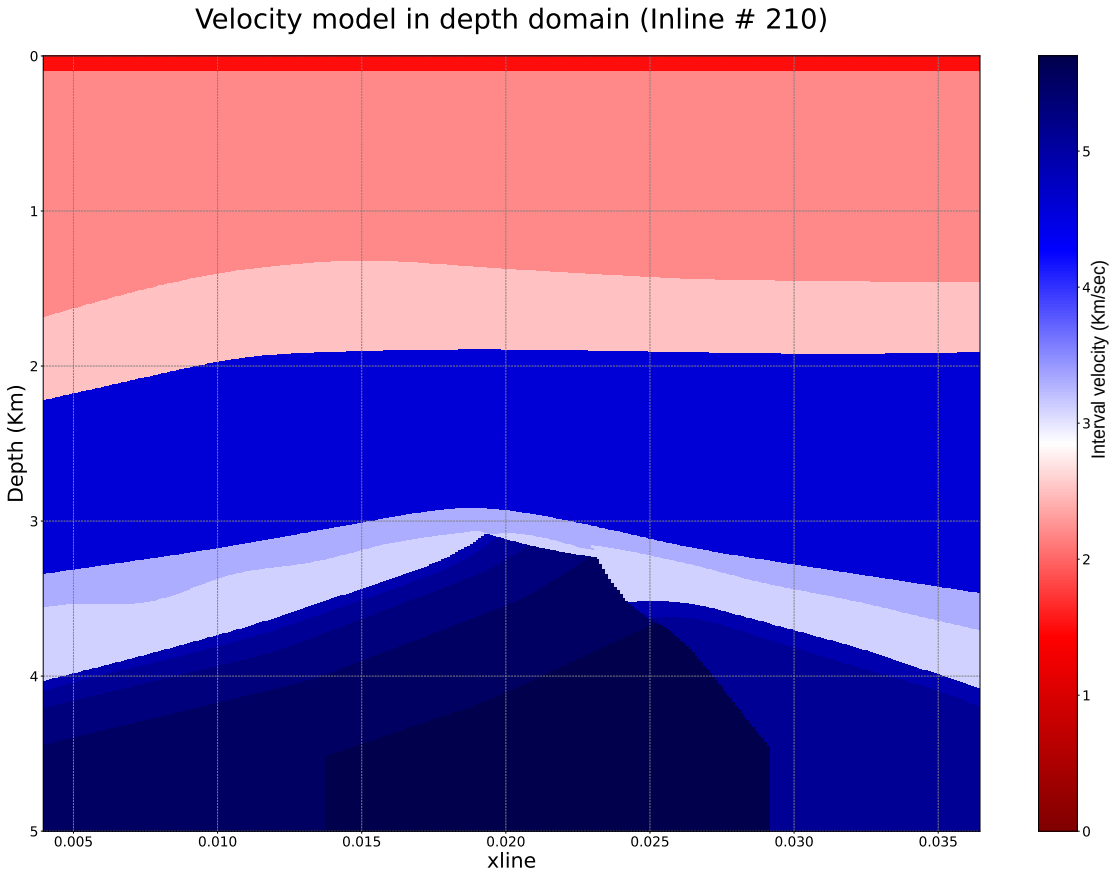

Figure 5.6: illustrate the updated velocity model during drilling. The velocities are updated through reverse VSP.

5.4 Depth Horizon

The TWT of the Top Upper Fulmar horizon is converted to the depth based on the updated velocity model. In the updated model, the velocities have been reduced and the horizon is migrated to a shallower depth. Figure 5.7 illustrates the depth horizons before and after updating the velocity model during the drilling of the well. An orange and blue horizon represents the depth horizon that has been converted through the initial and revised velocity models, respectively. As compared to the original well plan, the target horizon is expected to be shallower. This difference in depth between the two horizons is not constant. There is a relationship between the thickness variation of the velocity blocks above and the difference in the depth of the horizon. As the velocities in the Overburden, Paleocene, and Chalk Blocks are the same, the depth mapping of the horizon is not affected by these velocity blocks. The interval velocity is updated in the

Cromer Knoll and Upper Jurassic Shale, which have varying thicknesses towards their flanks. The CDPs of the target horizon moved to a shallower depth where the overburden blocks are thicker (at the flanks) as compared to CDPs where the overburden blocks are thinner or not present. As a result of depth updating, the shallowest CDP moved from 3.09km to 3.04km while the deepest CDP migrated from 4.07km to 3.88km. The effect of migration depends on the velocity changes and the thickness of the velocity blocks in the overburden. This updated horizon will reduce the uncertainty of the target horizon. The uncertainty in depth is now a function of the remaining velocity uncertainties between the TD of the well and the (deeper) target horizon.

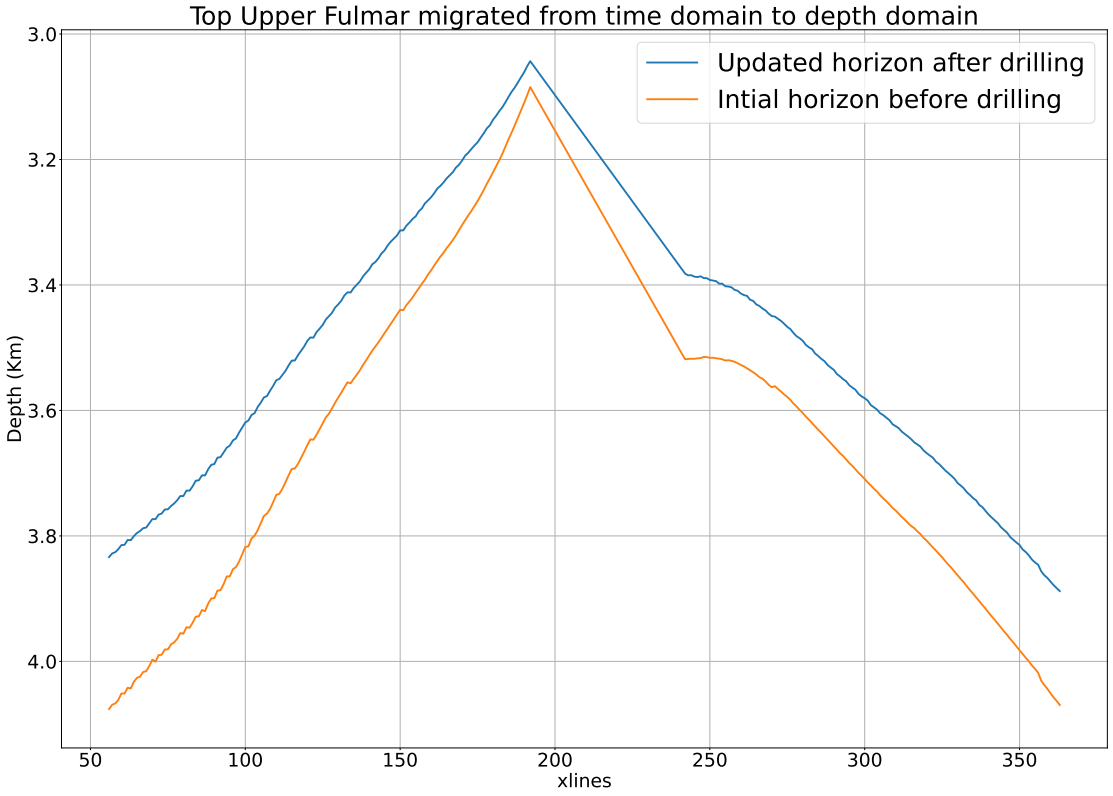

Figure 5.7: Represent migrated Top upper Fulmar horizon. The orange horizon is migrated with the initial velocity model while the blue represents the target horizon migrated with the updated velocity model.

5.5 Uncertainties affect

The new velocity updates the geological horizons, but errors are still expected. The goal is to obtain an uncertainty range that is less than the length of one drill pipe (10 m). This rises the question: how far is the target horizon and at what depth the velocity model should be updated to get the uncertainty within the threshold values? Updating the velocities much higher in TD will give a longer time to reach the target horizon and higher uncertainty in calculated depth. The uncertainty in depth is also translated from

input values. Uncertainty can be associated with the updated velocities or the remaining velocities to the target horizon. The second source of uncertainty can be a time associated with velocity. Uncertainty can also be originated from the interpretation of the geological horizon (TWT). The uncertainties are applied as random values through bootstrapping for uncertainties within a tolerance of 0.001 sec for time values (TWT, time associated with velocities). Similarly, 0.01 Km/sec standard deviation is applied to interval velocity values. The time-to-depth model is iterated 100 times with the bootstrapped values in order to calculate the range of depth variation.

These uncertainties are applied to updated velocity values but there will be more uncertainty associated with the undrilled section of the well. Figure 5.8 illustrates all realization points for the depth values related to cross-lines. Based on applied uncertainty, each dot represents a different value of depth. Depending on the input values from the random generator, depth values may vary between these points. This uncertainty in depth is actually translated from three variables used as input for the mapping model. Most of the depth points are concentrated around the actual depth values, except for some outliers associated with a few cross-lines. The application of confidence intervals limits these outliers. The error bars in Figure 5.9 and Figure 5.10 represent the confidence interval of 95% and 67% respectively. With a 95% confidence interval, 2.5% distribution

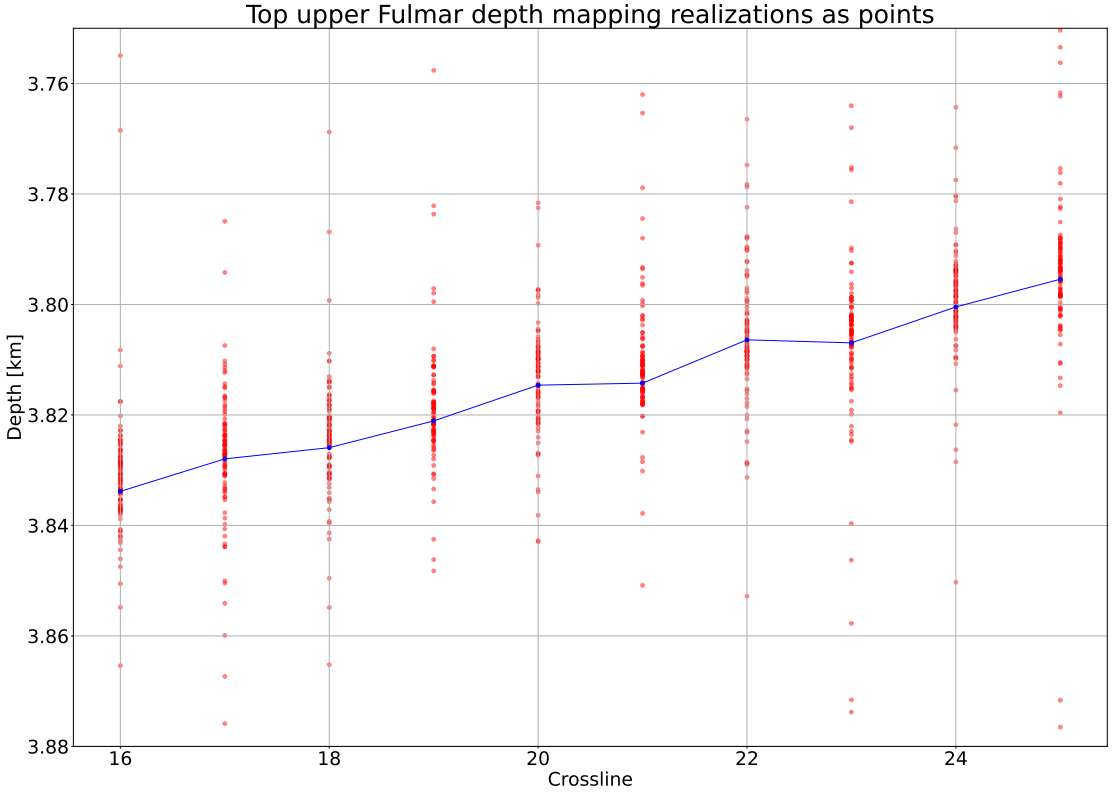

Figure 5.8: shows the depth realization points calculated by applying uncertainty and iterating it 100 times. For a better representation, only the first 10 cross-line are plotted.

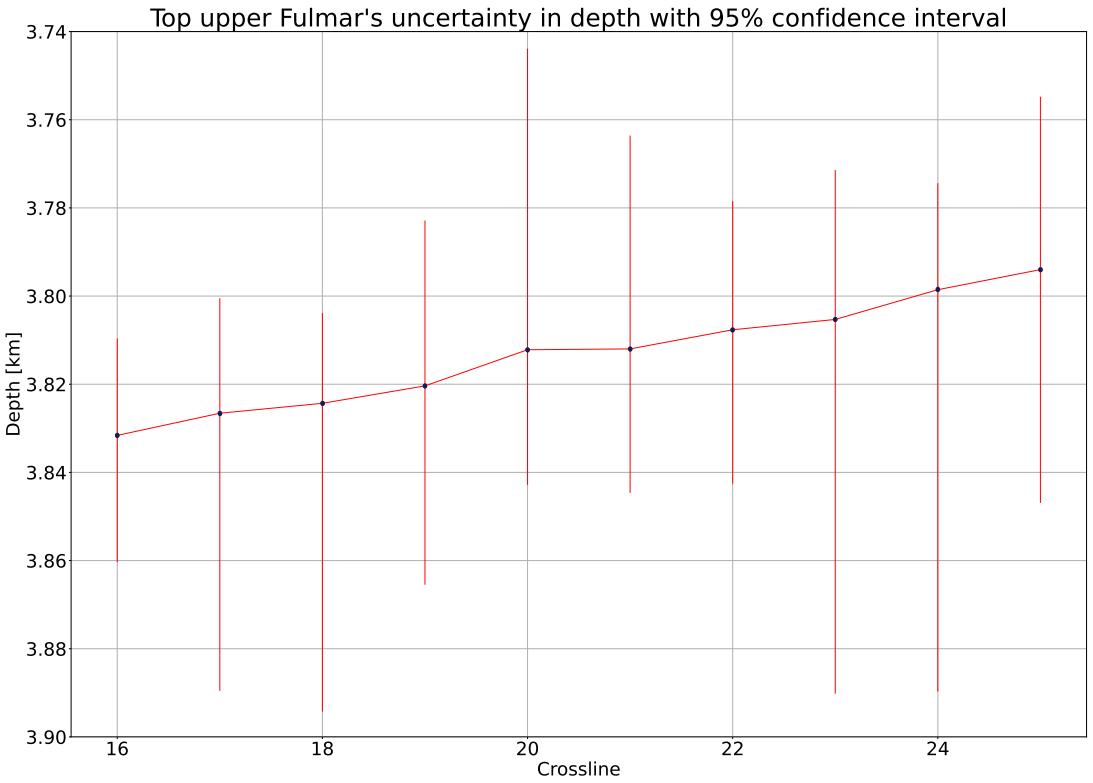

Figure 5.9: Represents the 95 percent confidence interval as error bars on the uncertainty in depth. For a better representation, only the first 10 crossline are plotted.

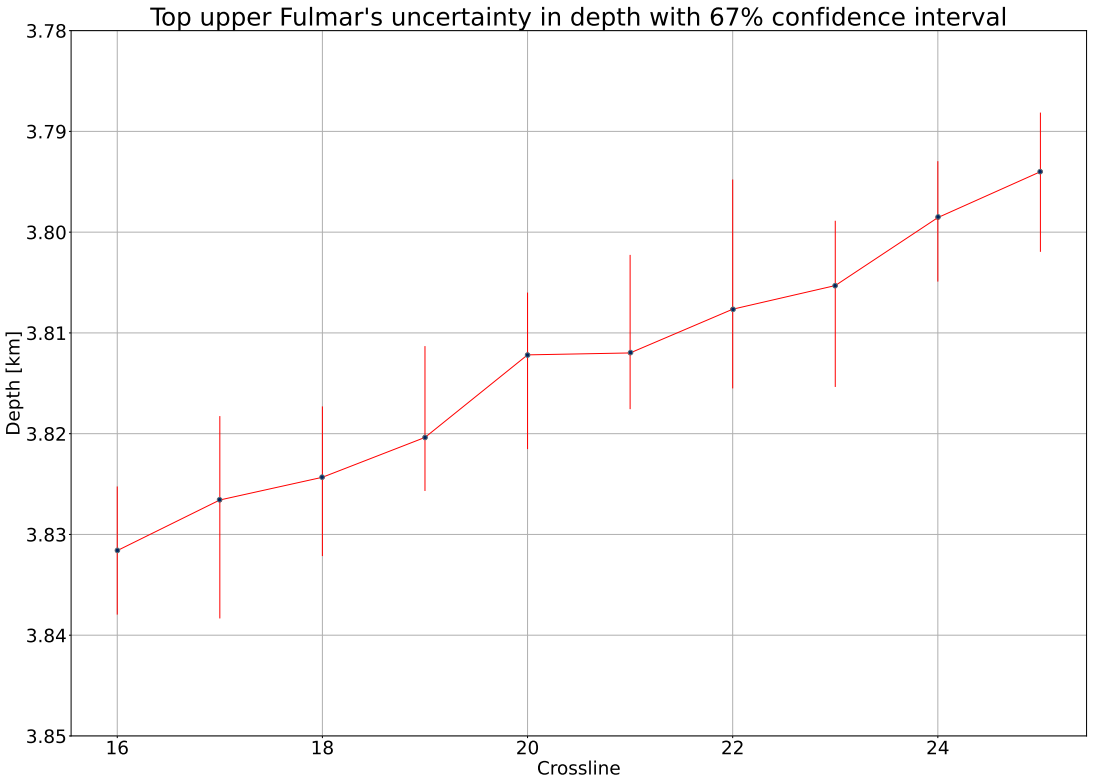

Figure 5.10: Represents the 60 Percent confidence interval as error bars on the uncertainty in depth. For a better representation, only the first 10 crossline are plotted.

is emitted from each side, while with a 67% confidence interval, 16.5% distribution is emitted. A 95% confidence interval indicates that there is a maximum deviation of 5 to 6 meters in the depth measured. A quantile range of 67% gives a more narrow range and indicates a maximum deviation of 3 meters in depth. The depth variation range is different at each cross-line.

Chapter 6

Discussion

In this chapter, we discuss the achieved results, factors affecting the performance of the proposed model, and the limitations of the thesis. This chapter also discusses the effects of preprocessing on model results.

6.1 Effectiveness of the proposed computational model

The computational model proposed in this thesis is based on specific algorithms that convert the TWT of the geological surface into depth. This computational model is divided into two parts. The first part takes the geological model and calculates the zero offset TWT of the target horizon. At this step, the geological model is sampled to create an input velocity model. These sampled values affect the efficiency of the time-to-depth model. A smaller sampling interval increases the efficiency of the computational model.

The second step is based on the algorithms that convert the TWT into depth. There is a great deal of sensitivity to the number of resampled values of interval velocities and their associated time in the model. The Comparison of calculated and reference depth values show better results with shorter resampling intervals. According to the computational model of time-to-depth conversion, the Top Upper Fulmar depth values can be calculated with more than 99% precision when more than half of the input velocity values are resampled. Reduced resampling interval increases the consistency between the resampled and input velocities which results in better depth estimation as shown in chapter 5.

The computational model is repeated with the updated velocities from the reverse VSP that updates the depth values beforehand. Still, uncertainty is expected in the updated depth values because of uncertainties associated with the VSP velocities and interpretation of the geological horizon (TWT). The depth uncertainty range calculated

through bootstrapping is still within the limits of the threshold values of the one drill pipe (10m).

6.2 Effect of pre-processing

The efficiency of the time-to-depth conversion model is also influenced by pre-processing. The most significant effect is caused by sampling the velocity model. It is evident that the computational model is more efficient when the sampling interval is short. With a smaller sampling interval, more values can be taken into account, which results in more accurate linear interpolation resampling. The efficiency is linked to the consistency of the resampled interval velocity and the input sampled values. In this thesis, the sampling interval is one meter on the z-axis, which generates 99% efficient results, while on the y-axis, sampled values have no effect because the initial model is 2.5D. The velocity model is sampled with 25 meters intervals because the library used to import the SEG-Y file does not work when the sampling interval is further reduced. Ideally, the calculated travel time should be zero offset as this is the shortest time for the ray to travel from the source to the target. Due to the fact that the model takes travel time in seconds and velocity in kilometers per second, the values must be exported in their respective units after pre-processing. Otherwise, these values must be converted into appropriate units.

6.3 Evaluation of the velocity models

For the time-to-depth conversion, the initial velocity model is based on stacking velocities. There is a significant error in estimating the velocities from surface seismic data and the error increases with depth. It is difficult to determine the inverse (reduction) in velocities based on the semblance plot. The error in velocity is translated into depth estimation. A reverse VSP approach is used during drilling for updating seismic velocities, using the seismic waves of the drill bit. This technique is helpful for looking ahead to the target horizon (Geortz et. al., 2021). In shallow blocks, the interval velocities are recorded the same as in the initial model, whereas, in deeper blocks, there is a considerable difference in the interval velocities. This revised velocity model converts the TWT of the target horizon to its accurate depth. The difference in velocities determines whether the horizon migrates shallower or deeper. In the case of lower velocities than the initial velocity, the migrated horizon will be shallower as shown in Figure 5.7. In a similar manner, if the velocity value is increased than the initial value, the horizon will migrate deeper.

The depth variation is not the same for each cross-line despite the updated velocity being the same in overburden blocks. The depth variation is affected by inconsistencies

in lateral thickness. The depth difference is higher where the overburdened blocks are thicker and vice versa.

Even with the updated velocity model, the target horizon depth cannot be estimated accurately. Uncertainties can be associated with either the input variables (travel time, interval velocities, and their associated times) or the interval velocities in the remaining section of the well. The uncertainty in the form of Gaussian error is translated into depth values, giving the range of depth variation. The target horizon can be present anywhere within the calculated depth range. Still, these ranges fall within the threshold value of one drill pipe. The uncertainty associated with the interval velocities of the remaining section of the well rises the question: at what depth of the well the velocity model is updated to keep the depth range within the threshold value of one drill pipe?

6.4 Limitations

This section will discuss some of the limitations of the proposed model.

6.4.1 Velocity model updating

The velocity model is updated through Reverse VSP, which provides interval velocities that are the closest to the actual velocities of the strata. The process of updating velocities does not take into account lateral variation in stratigraphy. Because the velocities are recorded in the vicinity of the well, the updated velocities will be accurate up to a few meters away from the well location. Depending on the lithology, the updated velocity model may be of limited value if lateral variations in velocities occur. The revised map of the target horizon using the updated velocity model will have an inaccuracy in the velocities away from the well.

6.4.2 Computational limitations

This method of mapping the time horizon to depth is efficient compared to other methods of time-to-depth conversion. Computation time is affected by the number of resampled values extracted from the velocity model. Increasing the number of values results in more accurate depth measurements, but it also takes a longer time. In addition, computation time depends on the number of CMP present in the study area. The reverse VSP velocity model provides information near the well. If it is assumed that there are no lateral variations in velocity, then TWT associated with all the CMPs in the project area can be utilized. The bigger project areas can increase computational time. In

addition, the computation of uncertainties through bootstrapping method is very time-consuming. Computational time can increase to hours depending upon the iterations. High computational power is needed for uncertainty calculation through bootstrapping.

The processing of reverse VSP data is also a time-consuming process. All of these factors may increase the computational time, which must not exceed the time required to drill the remaining section of the well to reach the target horizon. Depending on the drilling parameters and the lithology ahead, the time required to drill the section varies. There should be enough time to update the depth with reasonable resampled velocity values.

Chapter 7

Conclusion and Recommendations

This chapter concludes this thesis and provides recommendations for future research.

7.1 Conclusion

This thesis proposes a method of mapping the TWT of the target horizon to depth before and after velocity updates. The reverse VSP data recorded with a drill bit as the seismic source is the proposed method for updating the velocity model. This thesis deals with a specific input subsurface model that is pre-processed to calculate the TWT before actually using it in the mapping model. The interval velocities are integrated over time to calculate the depth before drilling the target horizon.

This thesis follows a two-step methodology in which the first step involves the pre-processing of the 2.5D earth model and the second step involves the mapping of the target horizon from time to depth before and after updating the velocity model. The pre-processing gives the flexibility of sampling the velocity model with different sampling intervals. The zero offset TWT of the target horizon is calculated through forward modeling using ray tracing theory. In this thesis, the designed computational model also does the mapping of the velocity model from depth to time. The velocity model is resampled in a way to ensure that the interval velocities are consistent with the input velocities. The results illustrate that the computation model works efficiently when more than half the values of the input velocity model are resampled. The TWT of the target horizon is converted to depth through the designed computational model before drilling the target horizon. The target horizon depth is calculated again with the updated velocity model. The depth variations estimated through bootstrapping are dependent on applied uncertainty to input parameters (TWT, Interval velocity, and its associated time

). By changing the values of applied uncertainty to the input parameters, a range of depth variation can be estimated. The remaining uncertainty is expected from interval velocities associated with the undrilled section of the well.

A set of experiments are performed to find the optimal resampling interval and authenticity of the time-to-depth conversion model. Based on the results of this thesis, it has been determined that the depth of the reservoir horizon can be updated in advance using the updated velocity model from the reverse VSP. The TWT of the target horizon is efficiently converted to depth through the designed computational model. In addition, a range of depth variations can also be predicted depending on the level of uncertainty.

To conclude, the obtained results support the primary aim of this thesis; that is, to develop a method for time-to-depth conversion of the target horizon to actual depth using the updated velocity model estimated through the VSP of the drill bit seismic without interrupting drilling. The calculation of zero offset TWT is also part of the thesis which is done through forward modeling.

7.2 Future Recommendations

With the advent of new technology, seismic measurements are becoming more and more relevant while drilling. Drill-bit seismic waves are being used as a source of VSP in the development of this method. As a result of reverse VSP, drilling costs and rig downtimes are being reduced. The process developed in this thesis is based on a 2.5D model of the earth. Additionally, this model can be extended to a 3D earth model, which will be more practical for real-world drilling operations. The extension of this model will enable the velocity model to be updated in three dimensions, which will be beneficial for future drilling operations.

This thesis has raised a question that needs to investigate to make the mapping model more efficient. what is the appropriate depth to update the velocity model to make sure the depth values are within the threshold values? The depth range calculated with uncertainties will be practical if they fall within the range of 10 meters (length of one drill pipe). So, the depth of the VSP is also an important aspect of further research.

The safe drilling of the well is another important issue that can be addressed with this method. By using the updated accurate velocity model, it will be possible to determine the pore pressure of the overburden within the well. In order to reduce the risk of abnormalities occurring during drilling, it is essential to have a thorough understanding of the pore pressure beforehand. With this advancement, it will be possible to estimate

the zones of under-pressure and over-pressure more accurately during drilling. This recorded VSP velocity can be used to develop a model that can quantify the abnormal zones beforehand. This will enable us to make the drilling process safer and more economical by planning out remedies in advance.

List of Figures

List of Tables

Appendix A

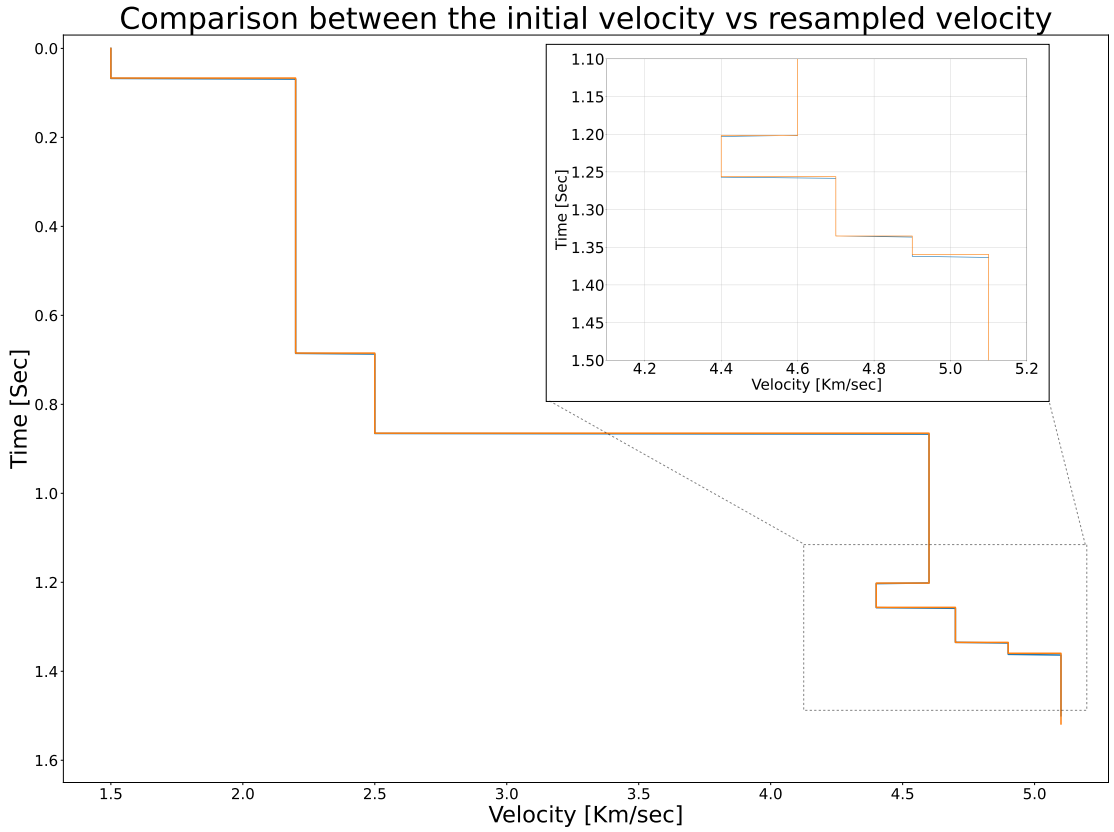

Figure A.1: Represent depths calculated from time to depth conversion model (orange) and extracted from software (blue). The depth is migrated with 1001 resampled interval velocity values.

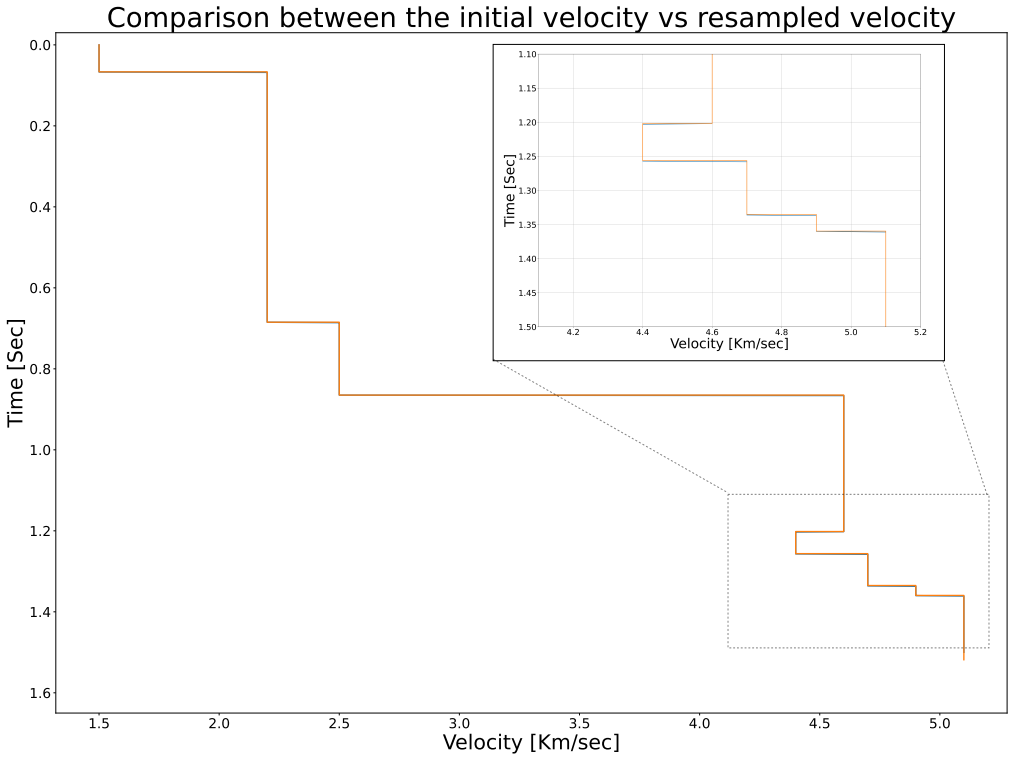

Figure A.2: Represent depths calculated from time to depth conversion model (orange) and extracted from software (blue). The depth is migrated with 1501 resampled interval velocity values.

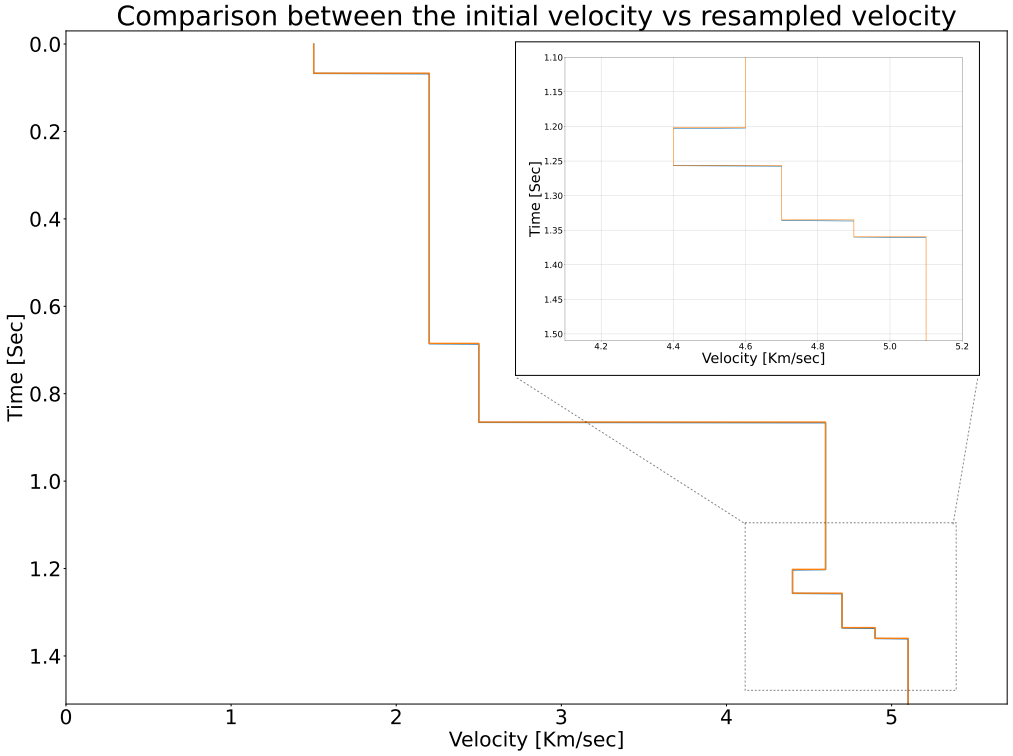

Figure A.3: Represent depths calculated from time to depth conversion model (orange) and extracted from software (blue). The depth is migrated with 2001 resampled interval velocity values.

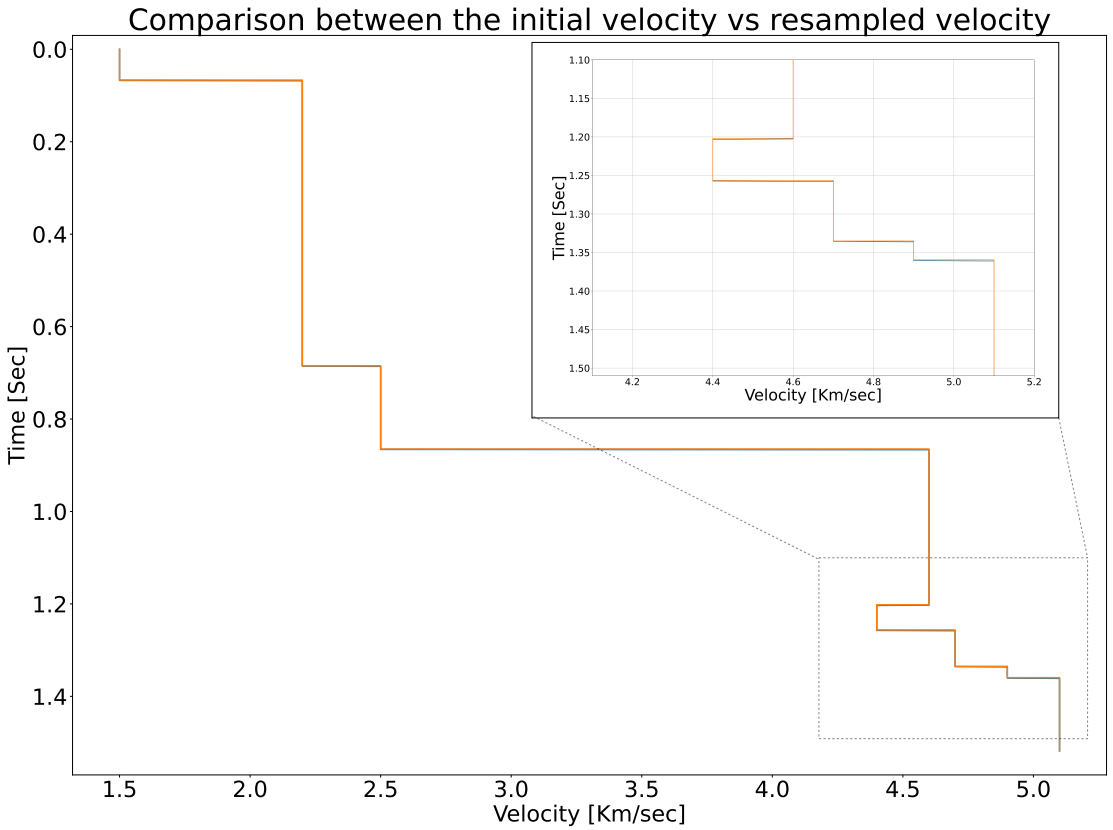

Figure A.4: Represent depths calculated from time to depth conversion model (orange) and extracted from software (blue). The depth is migrated with 2501 resampled interval velocity values.

Appendix B

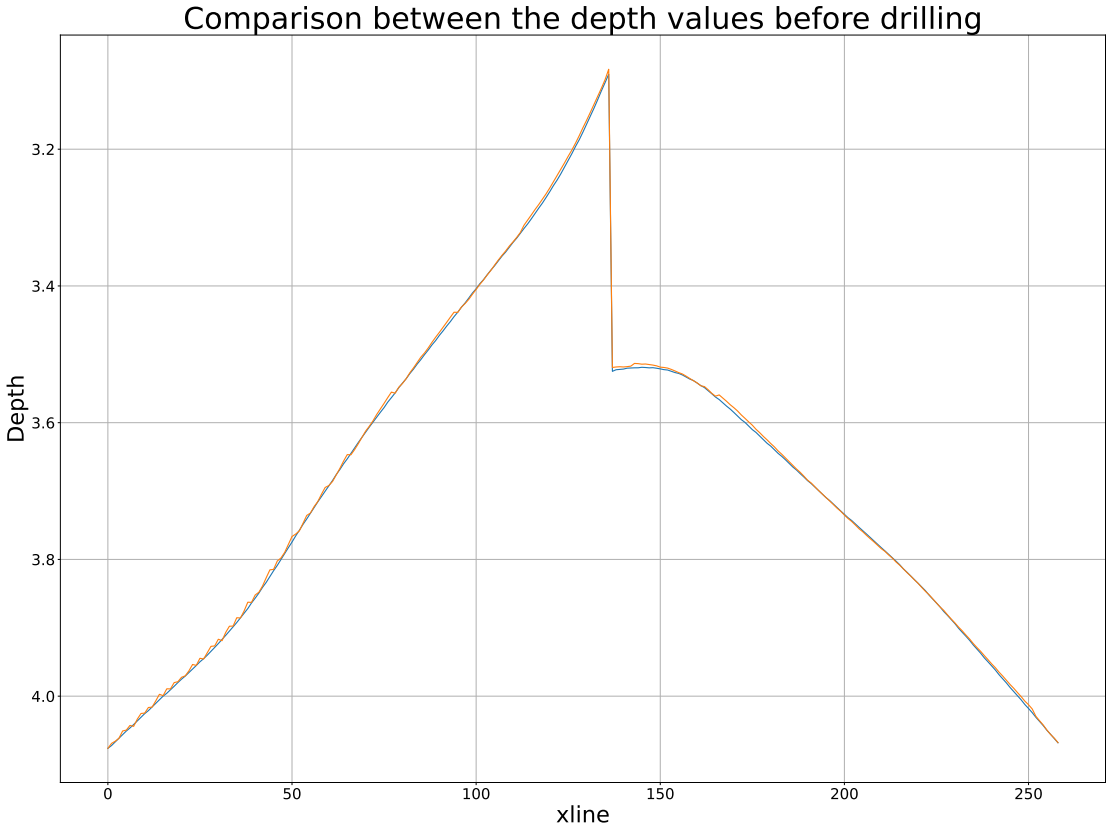

Figure B.1: Represent results from time-to-depth conversion (orange) with the original horizon (blue) obtained from NORSAR which serves as a reference. The depth is calculated with 1001 resampled velocity values.

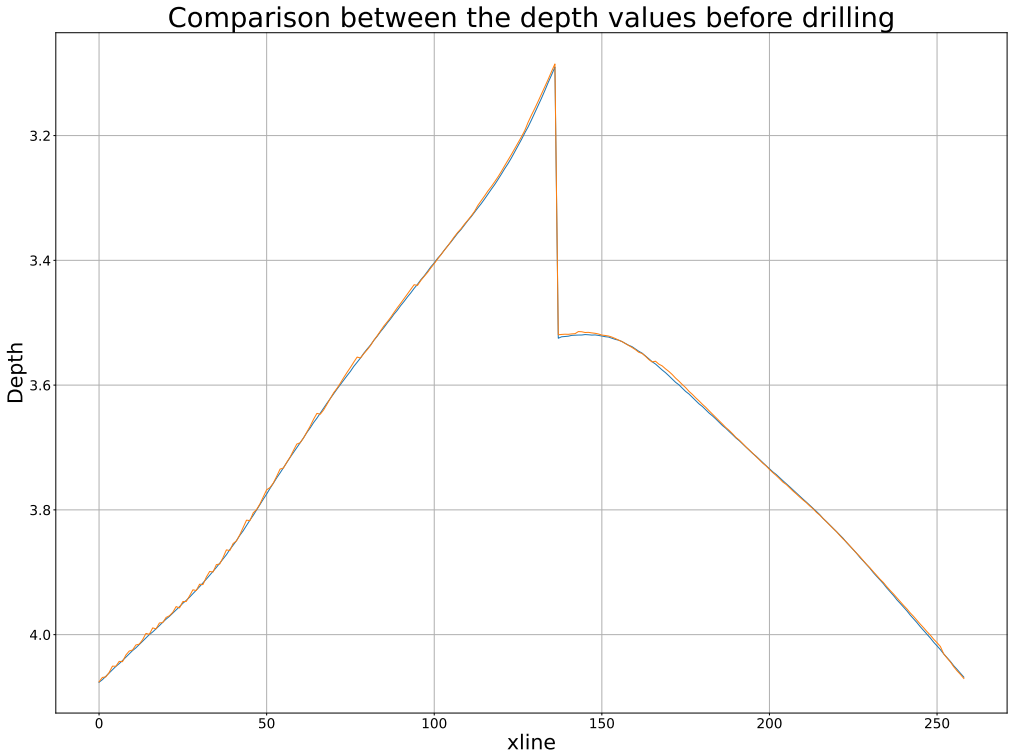

Figure B.2: Represent results from time-to-depth conversion (orange) with the original horizon (blue) obtained from NORSAR which serves as a reference. The depth is calculated with 1501 resampled velocity values.

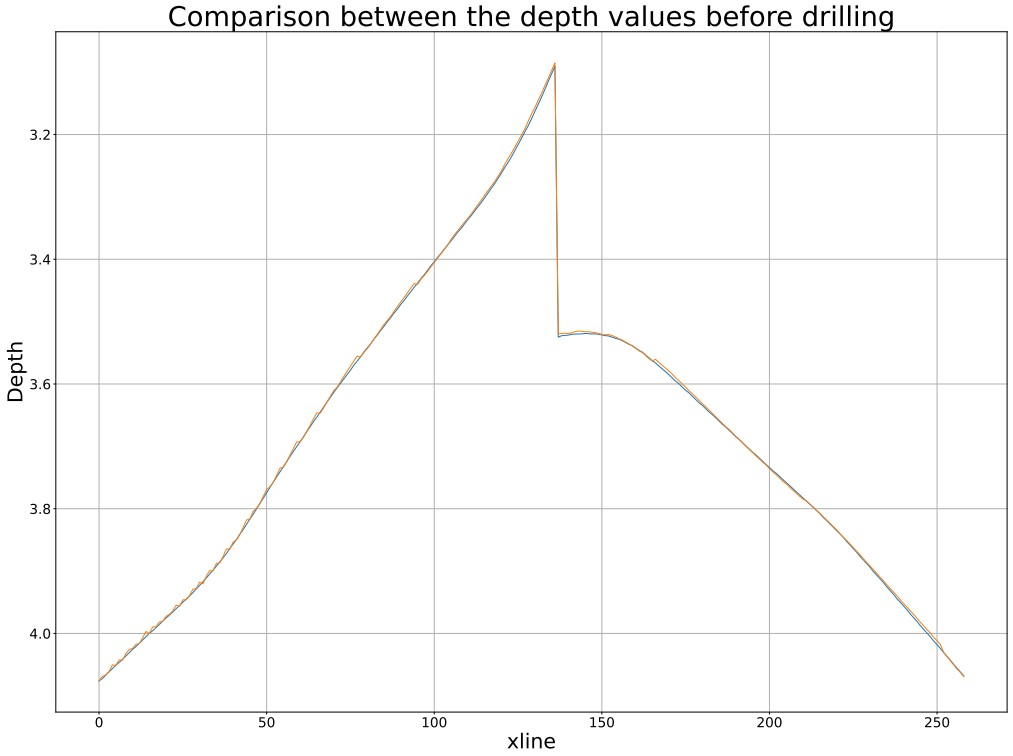

Figure B.3: Represent results from time-to-depth conversion (orange) with the original horizon (blue) obtained from NORSAR which serves as a reference. The depth is calculated with 2001 resampled velocity values.

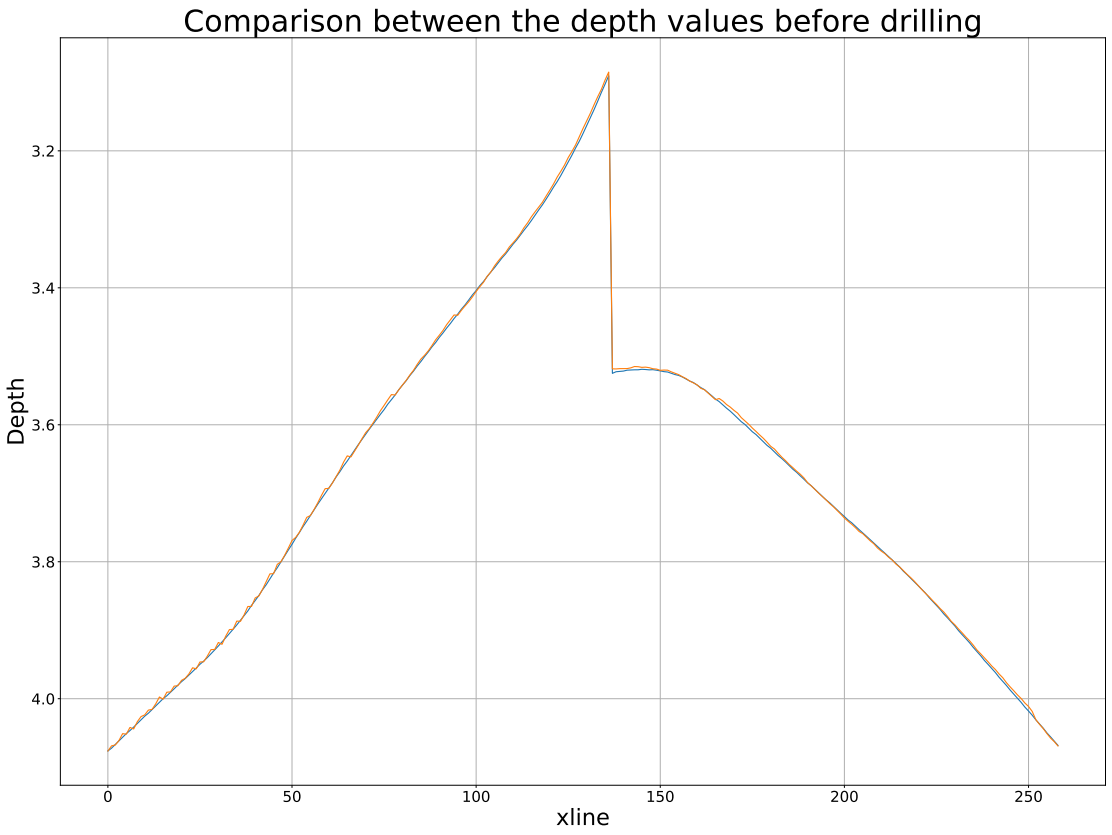

Figure B.4: Represent results from time-to-depth conversion (orange) with the original horizon (blue) obtained from NORSAR which serves as a reference. The depth is calculated with 2501 resampled velocity values.

Appendix C

Python Programming Code

The relevant Python code for all tasks performed in the thesis is present on the GitHub repository named "**Master_thesis**" and can be accessed using this link `https://github.com/muhammadusman-git/Forward-Model-for-Map-Migration.git` to the repository.

The explanation of used libraries and python code is present in the README.md file in the repository. The code will be publicly available after March 1st, 2023 due to copyright reasons.

Bibliography

[1] Öz Yilmaz. Seismic data analysis: Processing, inversion, and interpretation of seismic data, Jan 2001. URL `https://pubs.geoscienceworld.org/seg/books/book/2102/Seismic-Data-Analysis-Processing-Inversion-and`.

[2] Clare Bond. Uncertainty in structural interpretation: Lessons to be learnt. *Journal of Structural Geology*, 74, 03 2015. doi: 10.1016/j.jsg.2015.03.003.

[3] FB Poletto and Francesco Miranda. *Seismic while drilling: Fundamentals of drill-bit seismic for exploration*. Elsevier, 2004.

[4] Derman Dondurur. *Acquisition and processing of marine seismic data*. 2018.

[5] IAGC OGP. An overview of marine seismic operations. *International Association of Oil and Gas Producers*, 448, 2011.

[6] Brian E. Hornby, Jianhua Yu, John A. Sharp, Amal Ray, Yan Quist, and Carl Regone. Vsp: Beyond time-to-depth. *The Leading Edge*, 25(4):446–452, 2006. doi: 10.1190/1.2193224. URL `https://doi.org/10.1190/1.2193224`.

[7] Vijay K Arya and HD Holden. Deconvolution of seismic data-an overview. *IEEE Transactions on Geoscience Electronics*, 16(2):95–98, 1978.

[8] Wail Mousa and Abdullatif Al-Shuhail. *Processing of seismic reflection data using MATLAB™*, volume 5. 09 2011. doi: 10.2200/S00384ED1V01Y201109SPR010.

[9] Philip Kearey, Michael Brooks, and Ian Hill. *An introduction to geophysical exploration*, volume 4. John Wiley & Sons, 2002.

[10] Edwin S Robinson. Basic exploration geophysics. 1988.

[11] John M Reynolds. *An introduction to applied and environmental geophysics*. John Wiley & Sons, 2011.

[12] Edward L Etris, Nick J Crabtree, Jan Dewar, and Scott Pickford. True depth conversion: more than a pretty picture. *CSEG recorder*, 26(9):11–22, 2001.

[13] Mohamed A Rashed. Smart stacking: A new cmp stacking technique for seismic data. *The Leading Edge*, 27(4):462–467, 2008.

[14] Juan Wu and Min Bai. Fast principal component analysis for stacking seismic data. *Journal of Geophysics and Engineering*, 15(2):295, 2018.

[15] Ahmed Hussein and Ali Al-Rahim. *Noise Attenuation of 3D Seismic Cube in Al-Samawah Area South-west of Iraq.* PhD thesis, 03 2020.

[16] M. Farrell and R. Mersereau. On the impact of pca dimension reduction for hyperspectral detection of difficult targets: Semantic scholar, Jan 2005. URL `https://www.semanticscholar.org/paper/On-the-impact-of-PCA-dimension-reduction-for-of-Farrell-Mersereau/1fa570be607c79f5845ce4456509cdadd65a5037`.

[17] Jeno Gazdag and Piero Sguazzero. Migration of seismic data. *Proceedings of the IEEE*, 72(10):1302–1315, 1984.

[18] EA Robinson and S Treitel. Geophysical signal analysis: Society of exploration geophysicists. 2000.

[19] Mamdouh R Gadallah and Ray L Fisher. *Applied seismology: A comprehensive guide to seismic theory and application.* Number Sirsi) i9781593700225. 2005.

[20] R. W. England. Bacon, m., simm, r. redshaw, t. 2003. 3-d seismic interpretation. x 212 pp. cambridge, new york, melbourne: Cambridge university press. price £80.00 (hard covers). isbn 0 521 79203 7. *Geological Magazine*, 141(2), 2004. doi: 10.1017/S001675680422917X.

[21] Ashley Francis. A simple guide to depth conversion: Part ii. 2018.

[22] Muhamad Perdana, Sudarmaji Saroji, and Imam Gunawan. Seismic time to depth conversion and uncertainty analysis for horizon prediction in a proposed well-site of sungai gelam field, jambi sub-basin. 05 2013. doi: 10.29118/IPA.0.13.SG.057.

[23] Muhamad Perdana, Sudarmaji Saroji, and Imam Gunawan. Seismic time to depth conversion and uncertainty analysis for horizon prediction in a proposed well-site of sungai gelam field, jambi sub-basin. 05 2013. doi: 10.29118/IPA.0.13.SG.057.

[24] RE Sheriff and LP Geldart. Exploration seismology: Press syndicate of the university of cambridge, 592p. 1995.

[25] Alistair R. Brown. What is seismic interpretation?, May 2013. URL `https://explorer.aapg.org/story/articleid/2471/what-is-seismic-interpretation`.

[26] M. M. ROKSANDIĆ. Seismic facies analysis concepts *. *Geophysical Prospecting*, 26(2):383–398, 1978. doi: https://doi.org/10.1111/j.1365-2478.1978.tb01600.x. URL https://onlinelibrary.wiley.com/doi/abs/10.1111/j.1365-2478.1978.tb01600.x.

[27] Larisa V Branets, Sartaj S Ghai, Stephen L Lyons, and Xiao-Hui Wu. Challenges and technologies in reservoir modeling. *Communications in Computational Physics*, 6(1):1, 2009.

[28] Philip Ringrose and Mark Bentley. *Reservoir model design*. Springer, 2016.

[29] Michael J Pyrcz and Clayton V Deutsch. *Geostatistical reservoir modeling*. Oxford university press, 2014.

[30] N. Adams. Peh:introduction to well planning, Apr 2017. URL https://petrowiki.spe.org/PEH:Introduction_to_Well_Planning.

[31] J. Ogden and N. Johnson. 2 - techno-economic analysis and modeling of carbon dioxide (co2) capture and storage (ccs) technologies. In M. Mercedes Maroto-Valer, editor, *Developments and Innovation in Carbon Dioxide (CO2) Capture and Storage Technology*, volume 1 of *Woodhead Publishing Series in Energy*, pages 27–63. Woodhead Publishing, 2010. ISBN 978-1-84569-533-0. doi: https://doi.org/10.1533/9781845699574.1.27. URL https://www.sciencedirect.com/science/article/pii/B9781845695330500023.

[32] Alex Goertz, Brian Atkinson, Tatiana Thiem, Endre Vange Bergfjord, Magne Oldervoll, Jon Haugestaul, Gábor Kocsis, and Harald-André Knoop. Real-time lookahead imaging with drill-bit seismic in the central north sea. *First Break*, 39 (11):61–68, 2021.

[33] Carlos Piedrahita and Clara Montana. Methodology implemented for the 3d-seismic modelling using gocad and norsar 3d software applied to complex areas in the llanos foothills. *Journal of Earth Science*, 11:35–43, 07 2007.

[34] Vetle Vinje, Einar Iversen, and Håvar Gjøystdal. Traveltime and amplitude estimation using wavefront construction. *GEOPHYSICS*, 58:1157–1166, 08 1993. doi: 10.1190/1.1443499.

[35] Guido Van Rossum et al. Python programming language. In *USENIX annual technical conference*, volume 41, pages 1–36. Santa Clara, CA, 2007.

[36] KR Srinath. Python–the fastest growing programming language. *International Research Journal of Engineering and Technology*, 4(12):354–357, 2017.

[37] Stefan Van Der Walt, S Chris Colbert, and Gael Varoquaux. The numpy array: a structure for efficient numerical computation. *Computing in science & engineering*, 13(2):22–30, 2011.

[38] J. D. Hunter. Matplotlib: A 2d graphics environment. *Computing in Science & Engineering*, 9(3):90–95, 2007. doi: 10.1109/MCSE.2007.55.